hMSCs are reported to avoid allogeneic rejection when they are transplanted into rat brains in a model of ischemia (38). Here we show that the hMSCs can migrate to neuropathological lesions in prion-infected mice and that their transplantation prolongs the survival of such mice. In addition, we also show that hMSCs that have migrated to prion-specific lesions secrete trophic factors and differentiate into cells of neuronal and glial lineages.

MATERIALS AND METHODS

MSCs. A retroviral vector, Rx-LacZ-bsr, containing the expression units of the *lacZ* gene and a gene conferring blasticidin resistance, were generated as described elsewhere (63). The recombinant retrovirus was used to transfect human bone marrow-derived MSCs that had been immortalized with the human telomerase catalytic subunit gene (26), and hMSCs were selected in the presence of 10 μg/ml of blasticidin. hMSCs stably expressing β-galactosidase (β-Gal) were cultured with Dulbecco's modified Eagle medium (DMEM) (Sigma Chemical Co., St. Louis, MO) containing 10% fetal bovine serum under a humidified atmosphere of 5% CO_2 at 37°C.

Mice and prion inoculation. Animal experiments were performed according to protocols approved by the Institutional Committee for Animal Experiments. Four-week-old female Jcl:ICR mice were purchased from CLEA Japan, and all mice were acclimatized for a week prior to use. Mice were intracerebrally inoculated with 20 μl of a 10% (wt/vol) brain homogenate from Jcl:ICR mice infected with the scrapie strain Obihiro or Chandler. Mice assigned to the mock-infected group were intracerebrally inoculated with 20 μl of a 10% (wt/vol) brain homogenate from age-matched uninfected Jcl:ICR mice. All mice were maintained on ad libitum feed and water with a 12-h light/dark cycle.

Transplantation of hMSCs. For transplantation of cells into the hippocampus or thalamus, mice were anesthetized by intramuscular injection of xylazine (10 mg/kg) and ketamine (50 mg/kg) and were placed on a stereotaxic apparatus (Narishige, Japan). After a linear scalp incision, burr holes were drilled to accommodate stereotaxic placement into the left hippocampus (2.0 mm caudal and 2.1 mm lateral to the bregma; depth, 2 mm) or thalamus (2.0 mm caudal and 1.5 mm lateral to the bregma; depth, 3.2 mm). hMSCs (1×10^5 cells in 2 μl phosphate-buffered saline [PBS]) were transplanted over a period of 15 min using a Hamilton syringe with a 31-gauge needle set in a micromanipulator. For transplantation of hMSCs via a peripheral route, 1×10^6 hMSCs were injected intravenously through the tail vein.

Immunohistochemistry. Mouse brains were frozen in Tissue-Tek OCT compound (Sakura, Japan), and cryosections (10 μm thick) were prepared as described elsewhere (53). Coronal sections were dried and fixed with ice-cold methanol for 15 min. A mouse anti-β-Gal MAb (catalog no. Z3783; Promega, Madison, WI) was conjugated with Alexa Fluor 488 by using a protein labeling kit (Molecular Probes, Eugene, OR) for the detection of hMSCs by direct staining. The following antibodies were used for the detection of various tropic factors: rabbit polyclonal antibodies against nerve growth factor (NGF) (Santa Cruz Biotechnology, Santa Cruz, CA), brain-derived neurotropic factor (BDNF) (Chemicon, Temecula, CA), neurotrophin 3 (NT3) (Chemicon), and neurotrophin 4/5 (NT4/5) (Santa Cruz Biotechnology); a rabbit MAb against vascular endothelial growth factor (VEGF) (clone EP1176Y; Abcam, Cambridge, MA); and a mouse MAb against ciliary neurotropic factor (CNTF) (clone A-11; Santa Cruz Biotechnology). As neuronal markers, we used a mouse MAb against microtubule-associated protein 2 (MAP2) (clone HM-2; Sigma Chemical Co.) for neurons, rabbit polyclonal antibodies (Dako, Denmark) against glial fibrillary acidic protein (GFAP) for astrocytes, and a mouse MAb against cyclic nucleotide phosphodiesterase (CNPase) (clone 11-5B; Chemicon) for oligodendrocytes. All sections were incubated with primary antibodies for 1 h at 37°C. To detect trophic factors and neural markers, the sections were subsequently incubated with an Alexa Fluor 546-conjugated anti-mouse antibody or an Alexa Fluor 555-conjugated anti-rabbit antibody (Molecular Probes) for 1 h at room temperature. After a wash with PBS, sections were mounted with Vectashield containing propidium iodide or 4′,6-diamidino-2-phenylindole (DAPI; Vector Laboratories, Burlingame, CA) and were examined with a Nikon C1 laser confocal microscope. To exclude the possibility of nonspecific reactions between the Alexa Fluor 546-conjugated anti-mouse antibody and mouse tissues, we carried out the immunostaining without primary antibodies and confirmed that the level of nonspecific binding of the Alexa Fluor 546-conjugated anti-mouse antibody was negligible.

For the detection of PrP^{Sc} accumulation and astrocytosis, mouse brains were fixed in 10% formalin and embedded in paraffin. Coronal sections (thickness, 4 μm) were subjected to hematoxylin-eosin (HE) staining or immunohistochemistry as described elsewhere (17, 53).

Proliferation assay. To detect proliferating cells in the brain, 50 mg of bromodeoxyuridine (BrdUrd; Sigma Chemical Co.) per kg of body weight in PBS with 0.007 M NaOH was administered to mice intraperitoneally twice a day for a week. BrdUrd administration was initiated soon or 2 weeks after the transplantation of hMSCs into the hippocampus. Mice were sacrificed 24 h after the last BrdUrd administration, and the brains of these mice were then prepared for cryosectioning. The sections were pretreated with 2 M HCl for 30 min at 37°C, followed by a neutralization step with 0.1 M borate buffer for 15 min at room temperature. BrdUrd in nuclei was detected using a fluorescein isothiocyanate-conjugated anti-BrdUrd MAb (clone B33.1; Abcam).

Cell migration assay. Prion- or mock-infected mice were sacrificed at 120 days postinoculation (dpi), and the brains of these mice were homogenized to 20% in DMEM (Sigma Chemical Co.). The homogenates were centrifuged at 10,000 × *g* for 10 min at 4°C, and the resulting supernatants were filtered (pore size, 0.22 μm). The brain extracts were aliquoted and stored at −80°C until use. Migration of hMSCs to brain extracts was analyzed using a QCM 24-well colorimetric cell migration assay kit (Chemicon). The hMSCs (approximately 80% confluent) were starved by incubation with serum-free medium 1 day before use. Then hMSCs were harvested, and a cell suspension (5×10^4 cells) was added to the insert well. The lower chambers were supplied with serum-free DMEM containing 1.0 or 0.1% brain extract. Twenty-four hours after incubation, hMSCs that had migrated through the polycarbonate membrane were extracted, and the absorbance at 560 nm was measured according to the manufacturer's instructions.

RESULTS

Distribution of hMSCs to the neuropathological lesions of prion disease. To test if hMSCs migrate to brain lesions caused by prion infection, we transplanted hMSCs into the left hippocampi of prion- or mock-infected mice at 120 dpi and monitored the distribution of β-Gal-positive hMSCs at 2 days and 1, 2, and 3 weeks after transplantation. In mock-infected mice, hMSCs were detected in the left hippocampus (transplanted side), but few hMSCs were detected in the contralateral hippocampus at 2 days to 3 weeks after transplantation (Fig. 1a). In contrast, hMSCs were detected both on the transplanted sides and on the contralateral sides of the hippocampi of mice infected with strain Chandler even 2 days after transplantation. Thereafter, hMSCs were constantly observed on both sides of the hippocampus during the observation period (every week after transplantation up to 3 weeks [Fig. 1a]). For each experimental group, we examined three mice at each time point and confirmed the similar results. One to 3 weeks after transplantation, hMSCs were also detected in the cortices, cerebella, medullae oblongatae (see Fig. 3b), and thalami (data not shown) of mice infected with prions, where intense PrP^{Sc} accumulations and astrocytosis were observed (see Fig. S1 in the supplemental material). Ramified hMSCs were observed in the corpus callosum; their morphologies differed from those observed in the contralateral hippocampus (Fig. 1b).

Transplantation of hMSCs into the left thalamus led to similar results. In mock-infected mice, hMSCs remained in the transplanted area, and few hMSCs migrated to the contralateral thalamus or to other regions. In contrast, many hMSCs were detected in the contralateral thalami (Fig. 1c) and hippocampi (data not shown) of mice infected with prions by 3 weeks posttransplantation.

We noticed a striking difference in the neuropathology of the hypothalami of mice infected with strain Obihiro versus strain Chandler. Specifically, PrP^{Sc} accumulations, astrocytosis, and spongiosis in the hypothalami of mice infected with

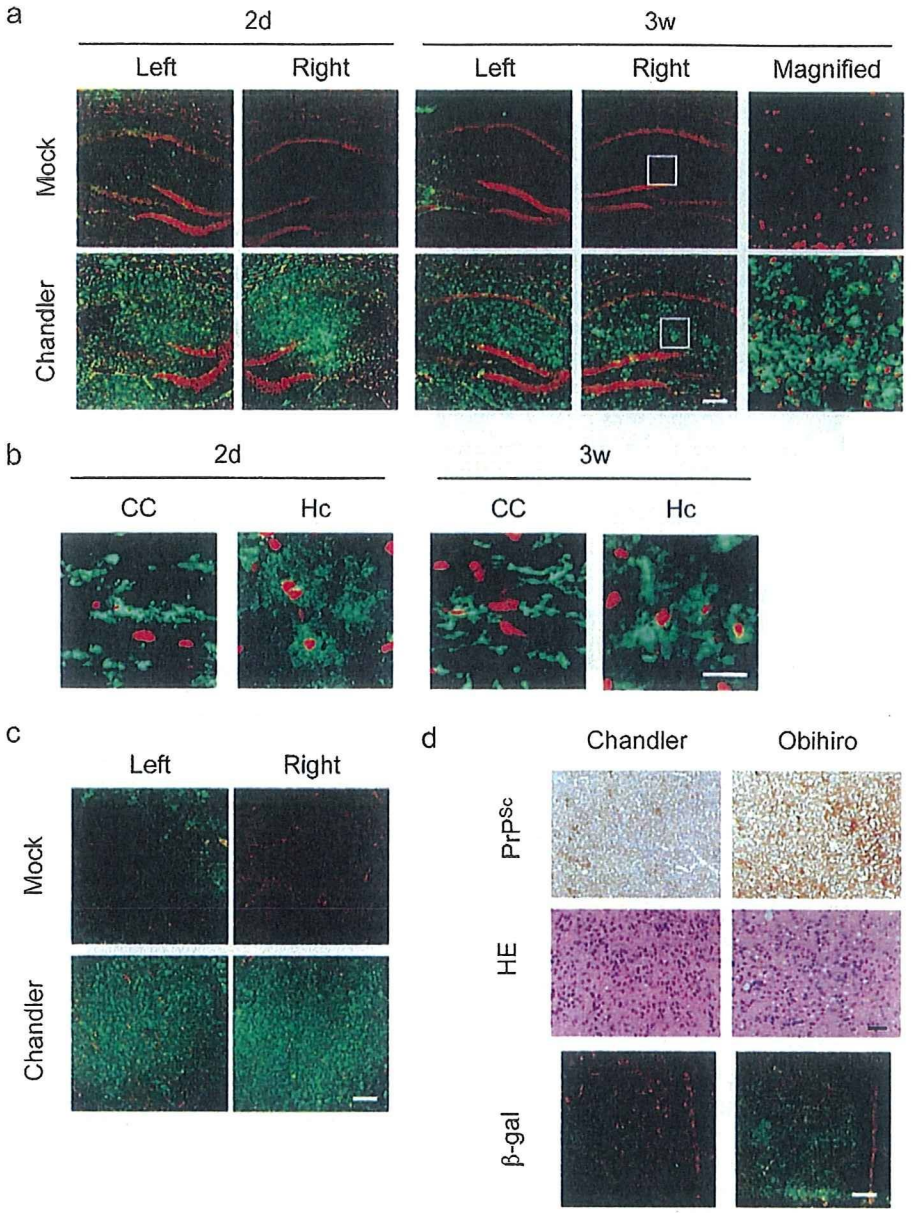

FIG. 1. Distribution of hMSCs to the neuropathological lesions of prion disease. At 120 dpi, hMSCs (1×10^5 cells) were transplanted into the left hippocampi or thalami of mice infected with strain Chandler and into those of age-matched mock-infected mice. Mice were sacrificed at 2 days or at 1, 2, or 3 weeks posttransplantation. Cryosections were stained with an Alexa Fluor 488-conjugated anti-β-Gal MAb (green) and counterstained with propidium iodide (red). (a) hMSCs in the hippocampus. Ipsilateral (left) and contralateral (right) hippocampi 2 days (2d) and 3 weeks (3w) posttransplantation are shown. The rightmost panels show magnified images of the regions boxed in the panels immediately to the left. Bar, 200 μm. (b) Morphology of hMSCs in the corpora callosa (CC) and contralateral hippocampi (Hc) of mice infected with strain Chandler at 2 days and 3 weeks posttransplantation. Bar, 20 μm. (c) hMSCs in the thalamus. Ipsilateral (left) and contralateral (right) thalami 3 weeks posttransplantation are shown. Bar, 200 μm. (d) Migration of hMSCs to the hypothalamus. (Top and center) Results of immunostaining for PrP^{Sc} and HE staining of the hypothalami of mice infected with strain Obihiro or Chandler are shown at 150 dpi. Bar, 100 μm. (Bottom) The hMSCs were detected in the hypothalamus (β-Gal) 3 weeks after transplantation into the left hippocampus. Bar, 200 μm.

strain Obihiro are more severe than those for mice infected with strain Chandler (Fig. 1d; see also Fig. S1 in the supplemental material). Consistent with the severity of neuropathological lesions, more hMSCs migrated to the hypothalami of mice infected with strain Obihiro than to those of mice infected with strain Chandler (Fig. 1d; β-Gal). These results suggest that hMSCs are capable of migrating to brain lesions caused by prion infection.

Migration of hMSCs in response to prion-specific lesions. To confirm the migration of hMSCs to lesions where PrP^{Sc} accumulates, we transplanted hMSCs into the left hippocampi of mice infected with strain Chandler at 73, 100, and 120 dpi, and we analyzed their migration to the contralateral (right) side a week after transplantation. When hMSCs were transplanted at 73 dpi, many hMSCs were detected on the transplanted side but fewer hMSCs were detected in the contralat-

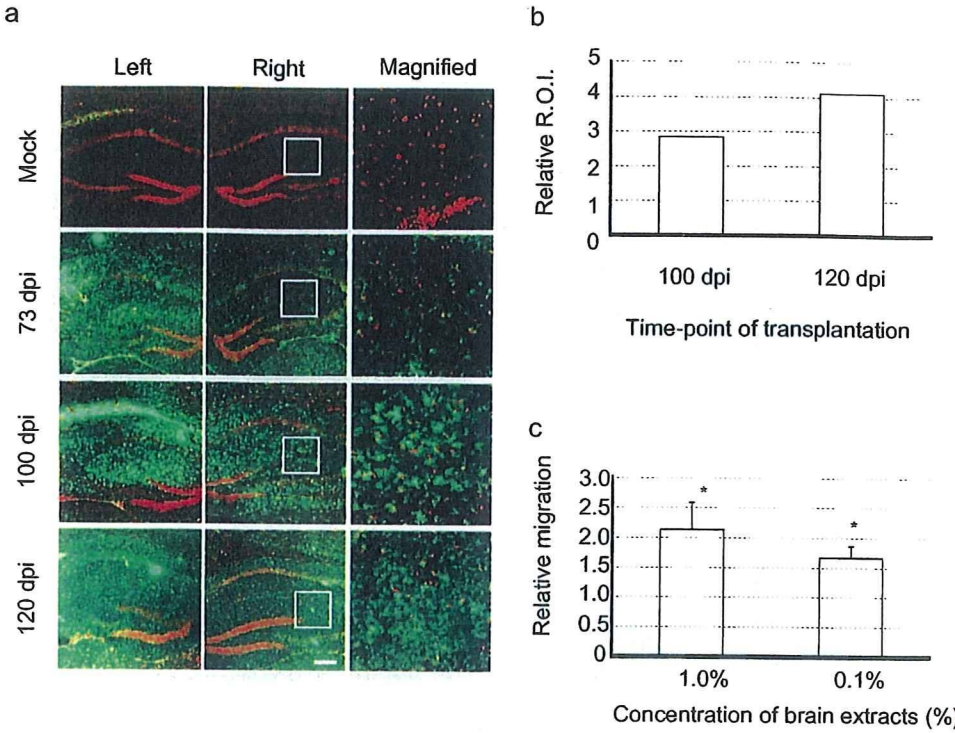

FIG. 2. Migration of hMSCs in response to prion-specific lesions. hMSCs (1×10^5 cells) were transplanted into the left hippocampi of mice infected with strain Chandler at 73, 100, or 120 dpi and into those of mock-infected mice at 120 dpi. One week after transplantation, the migration of hMSCs (green) to the contralateral hippocampus (right) was analyzed. The rightmost panels show magnified images of the regions boxed in the panels immediately to the left. Bar, 200 μm. (b) Quantification of hMSC migration. Areas positive for β-Gal in the contralateral hippocampus (regions of interest [ROI]) were measured using NIH Image J. The graph shows the levels of ROIs for mice transplanted at 100 and 120 dpi relative to that for a mouse transplanted at 73 dpi. (c) Migration of hMSCs to extracts from the brains of prion-infected mice. Insert wells containing an hMSC suspension were placed in the lower chambers, which contained 1.0 or 0.1% brain extract in serum-free DMEM, and were incubated for 24 h. The mean migration of hMSCs to brain extracts from mock-infected mice was arbitrarily set at 1, and the relative migration to brain extracts from mice infected with strain Chandler is indicated. Means and standard deviations from three independent assays (triplicate in each assay) are shown. *, $P < 0.05$.

eral hippocampus. In contrast, migration of hMSCs to the thalamus, where moderate PrP^{Sc} deposition had already occurred, was clearly observed (data not shown). In addition, more hMSCs were detected in the contralateral hippocampus when the transplantation was carried out at later time points (Fig. 2a). To compare the migration of hMSCs quantitatively, the total area of the hMSCs in the contralateral hippocampus (areas positive for β-Gal) was measured using the NIH Image J program. Compared to the migration of hMSCs to the contralateral hippocampus a week after the transplantation at 73 dpi, 2.8 and 4.1 times more hMSCs were detected when the transplantation was done at 100 and 120 dpi, respectively (Fig. 2b). We examined at least two mice from each experimental group and confirmed the consistency of the findings. Since PrP^{Sc} accumulation and astrocytosis in the hippocampi of mice infected with strain Chandler were first detected around 90 dpi and the levels of PrP^{Sc} accumulation and astrocytosis increased gradually thereafter (see Fig. S1 in the supplemental material), the migration of hMSCs to the contralateral hippocampus appeared to correlate with the severity of pathological changes.

Next, we analyzed the migration of hMSCs to brain extracts from prion-infected mice in vitro. Insert wells of a QCM 24-well colorimetric cell migration assay kit containing hMSCs were placed in the lower chambers, which contained 1.0 or 0.1% brain extract from prion- or mock-infected mice, and were incubated for 24 h. Cells that had migrated to the back sides (facing the lower chamber) of the membranes of the insert wells were quantified according to the supplier's instructions. Compared to the migration to brain extracts from mock-infected mice, approximately 2 and 1.5 times more hMSCs had migrated into the lower chambers containing 1.0% and 0.1% brain extracts from prion-infected mice, respectively (Fig. 2c). This suggests that chemoattractive factors that promote the migration of hMSCs are produced by the lesion caused by prion infection.

Migration of hMSCs into the brain after intravenous transplantation. MSCs have been reported to migrate to a site of brain injury even when they are introduced via intravenous injection (37, 38). To test if a similar phenomenon could be observed in prion-infected mice, hMSCs were intravenously inoculated into mice infected with strain Chandler or into mock-infected mice at 120 dpi. In mice infected with strain Chandler, hMSCs were observed in the hippocampus and thalamus even at 2 days after transplantation (data not shown). The cells showed a symmetrical distribution and appeared to increase in number in these tissues by 3 weeks posttransplantation (Fig. 3a; see also Fig. S2 in the supplemental material). In contrast, few MSCs were detected in the brains of mock-

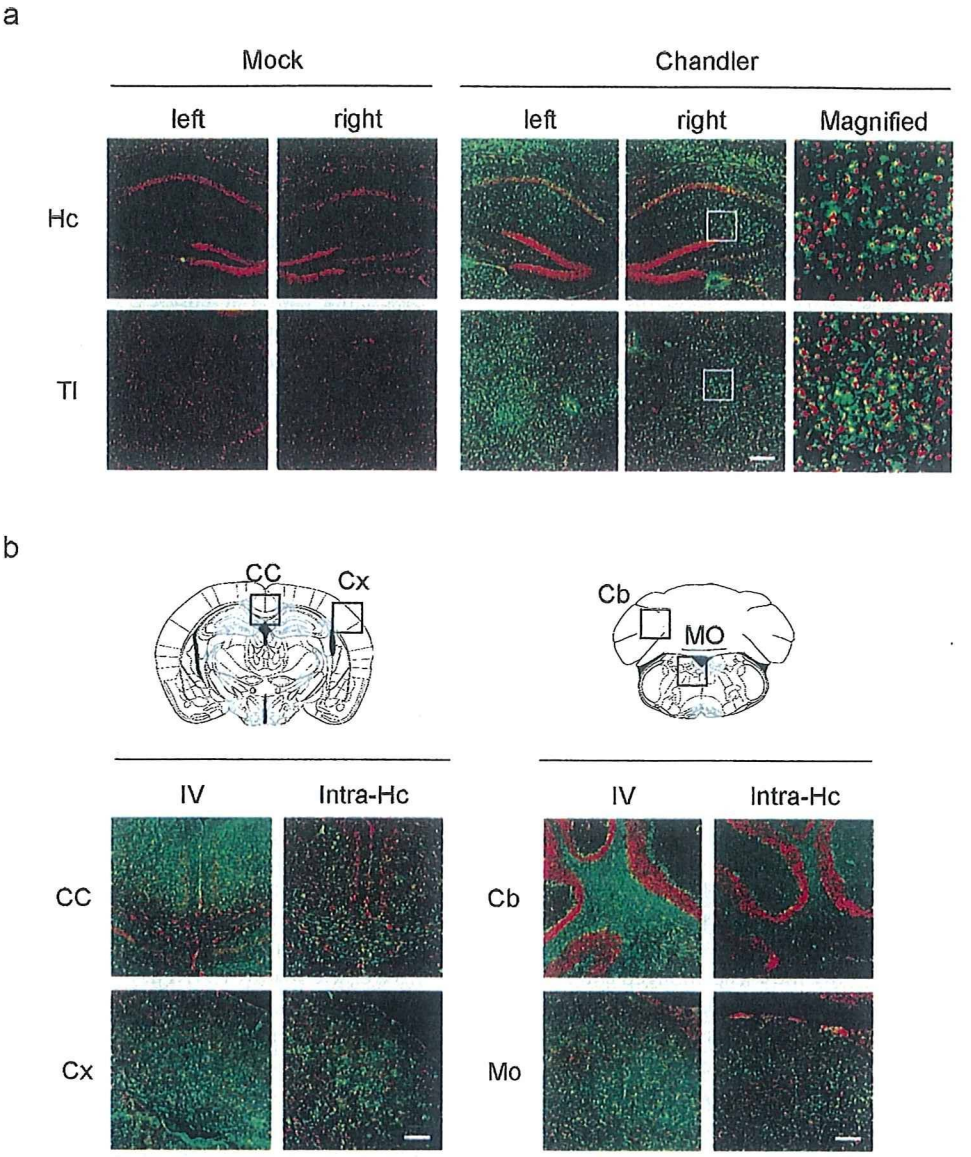

FIG. 3. Migration of hMSCs into the brain after intravenous transplantation. hMSCs (1×10^6 cells) were intravenously injected into mice infected with strain Chandler and into mock-infected mice at 120 dpi. Three weeks after injection, cryosections were prepared and stained with an anti-β-Gal MAb. (a) Presence of hMSCs in the left and right hippocampus (Hc) and thalamus (Tl) 3 weeks postinjection. The rightmost panels show magnified images of the regions boxed in the panels immediately to the left. Bar, 200 μm. (b) Distribution of hMSCs transplanted into the left hippocampus (Intra-Hc) or introduced via intravenous injection (IV). At 120 dpi, the hMSCs were transplanted into the left hippocampi (1×10^5 cells) or injected via the tail veins (1×10^6 cells) of mice infected with strain Chandler. The presence of hMSCs in the corpus callosum (CC), cortex (Cx), cerebellum (Cb), and medulla oblongata (MO) 3 weeks posttransplantation is shown. These brain regions are boxed on the images taken from Paxinos and Franklin and reprinted with permission of the publisher (39). Bars, 200 μm.

infected mice, demonstrating that the hMSCs migrated to the brain lesions caused by prion propagation. At each time point, we examined two mice for each experimental group and confirmed the consistency of the findings. The hMSCs were also well distributed in other brain regions, including the cerebral cortex, cerebellum, and medulla oblongata (Fig. 3b); however, consistent with the results shown in Fig. 3b, they did not migrate well to the hypothalamus (see Fig. S2 in the supplemental material). There was no difference in the area of hMSC distribution following intravenous versus intrahippocampal transplantation except at the corpus callosum. More hMSCs were observed in the corpus callosum after transplantation into the hippocampus than after intravenous injection, suggesting that cells migrate to the contralateral side through the corpus callosum after intrahippocampal transplantation (2).

Effects of transplantation of hMSCs on the survival of prion-infected mice. To examine whether the transplantation of hMSCs can ameliorate prion diseases, hMSCs were transplanted into the left hippocampi of mice infected with strain Chandler at 90 dpi. Figure 4 shows the survival curve for these mice. The intrahippocampal transplantation of hMSCs prolonged the survival of mice infected with strain Chandler

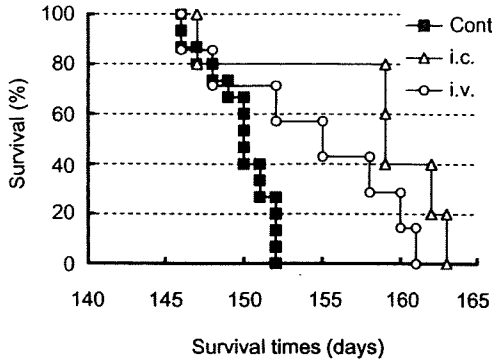

FIG. 4. Prolongation of survival of prion-infected mice by transplantation of hMSCs. For intracerebral (i.c.) transplantation, hMSCs (1×10^5 cells) were transplanted into the left hippocampi of mice infected with strain Chandler at 90 dpi ($n = 5$). For intravenous (i.v.) transplantation, 1×10^6 hMSCs were injected via the tail vein at 120 dpi ($n = 7$). The hMSC-transplanted and nontransplanted control (Cont) ($n = 15$) mice were observed until they reached the terminal stage of the disease. The graph shows survival curves.

(158 ± 6 days; $n = 5$) over that of the nontransplanted control group (150 ± 2 days; $n = 15$). Thus, hMSC transplantation prolonged mean survival by only 8 days, but this difference was statistically significant ($P < 0.01$ by the log rank test). We also transplanted hMSCs via the tail veins of mice infected with strain Chandler at 120 dpi. The transplantation of hMSCs via this peripheral route appeared not to be effective for nearly half of the mice; however, the remaining mice survived beyond the mean survival of the nontransplanted control group. Although the mean survival of hMSC-transplanted mice (154 ± 6 days; $n = 7$) was only a little longer than that of the control group, this difference was also significant ($P < 0.05$ by the log rank test). The fact that survival time was prolonged even when hMSCs were transplanted via a peripheral route after clinical onset (120 dpi) suggests that hMSCs have therapeutic potential for prion diseases. Since both intracerebral and intravenous transplantation of hMSCs prolonged the survival of prion-infected mice, we further analyzed the transplanted hMSCs.

Proliferation of hMSCs after transplantation. To examine the proliferation state of hMSCs that had migrated to lesions, BrdUrd was systemically administered after the transplantation of hMSCs to the left hippocampus. Three weeks posttransplantation, many BrdUrd-labeled nuclei were detected in the contralateral hippocampi and thalami of mice infected with strain Chandler (see Fig. S3 in the supplemental material), where many hMSCs had migrated (Fig. 1a). In contrast, few BrdUrd-labeled nuclei were detected in the contralateral hippocampi and thalami of mock-infected mice (see Fig. S3 in the supplemental material), although a few cells with BrdUrd-labeled nuclei were detected on the transplanted side (data not shown). BrdUrd-labeled cells were also observed in the cerebella and medullae oblongatae of mice infected with strain Chandler (data not shown). We examined two mice for each experimental group and confirmed the similar results. These results suggest that transplanted hMSCs are capable of proliferating in the microenvironment caused by prion propagation.

Expression of trophic factors in hMSCs. It is known that MSCs migrate to a site of injury in the brain and produce various trophic factors (8, 29). To ask if something similar happens in the case of prion disease, we next assayed the production of trophic factors in our model system. hMSCs were transplanted into the left thalamus at 120 dpi, and one mouse in each group was sacrificed and examined for the production of human trophic factors at 2 days and 1 and 3 weeks after transplantation. Immunoreactivities for human BDNF, NT3, and VEGF in the ipsilateral thalami of mice infected with strain Chandler became more intense from 2 days to 3 weeks posttransplantation. In contrast, no obvious increases, but rather decreases, in the signals of these trophic factors were observed for mock-infected mice (Fig. 5). Additionally, the expression of NGF, NT4/5, and CNTF was also upregulated (data not shown). These results suggest that hMSCs produce a variety of trophic factors in response to the neurodegeneration caused by prion infection.

Interestingly, only subpopulations of the hMSCs appeared to be positive for NT3 and BDNF. In addition, parts of the regions positive for these factors did not overlap with β-Gal staining. Since these antibodies are specific to human trophic factors and will not react with the corresponding mouse trophic factors, the presence of NT3 and BDNF in areas negative for β-Gal may represent trophic factors secreted from hMSCs and bound to mouse brain cells.

Differentiation of hMSCs. MSCs are known to differentiate into cells of neuronal and glial lineages in vivo and in vitro (11, 48, 61). We next asked if hMSCs differentiate into neuronal and glial cells in response to the lesions of prion diseases. At 3 weeks after transplantation into the thalamus, hMSCs positive for the neurodifferentiation marker MAP2, GFAP, or CNPase were detected in the brains of mice infected with strain Chandler (Fig. 6), although a relatively small number of hMSCs were positive for each marker. In contrast, no hMSCs positive for MAP2, GFAP, or CNPase were observed in the brains of mock-infected mice (data not shown), suggesting that neuronal and glial differentiation of hMSCs occurs in response to the neurodegeneration caused by prion infection. The GFAP-positive hMSCs were detected in the hippocampus, thalamus, and medulla oblongata. In contrast, MAP2-positive hMSCs were detected primarily in the hippocampus, cortex, and cerebellum, and CNPase-positive hMSCs were detected mainly in the cortex (data not shown).

DISCUSSION

The primary purpose of this study was to evaluate the potential of MSCs for treating prion diseases in a mouse model. For this purpose, the use of mouse MSCs would have been desirable; however, no appropriate method for the isolation of mouse MSCs from bone marrow had been established by the beginning of this study. On the other hand, it was well known that MSCs avoid allogeneic rejection (47). Thus, we adopted hMSCs to the mouse model and showed that hMSCs responded to the neuropathological lesions of prion diseases and may have therapeutic potential. Transplantation of MSCs is known to ameliorate neurological dysfunctions in experimental models (7, 23, 24, 30, 37). In clinical trials in which autologous MSCs are transplanted into patients with multiple system atrophy (28) or amyotrophic lateral sclerosis (33), or into patients who have suffered a stroke (3), there is some evidence of

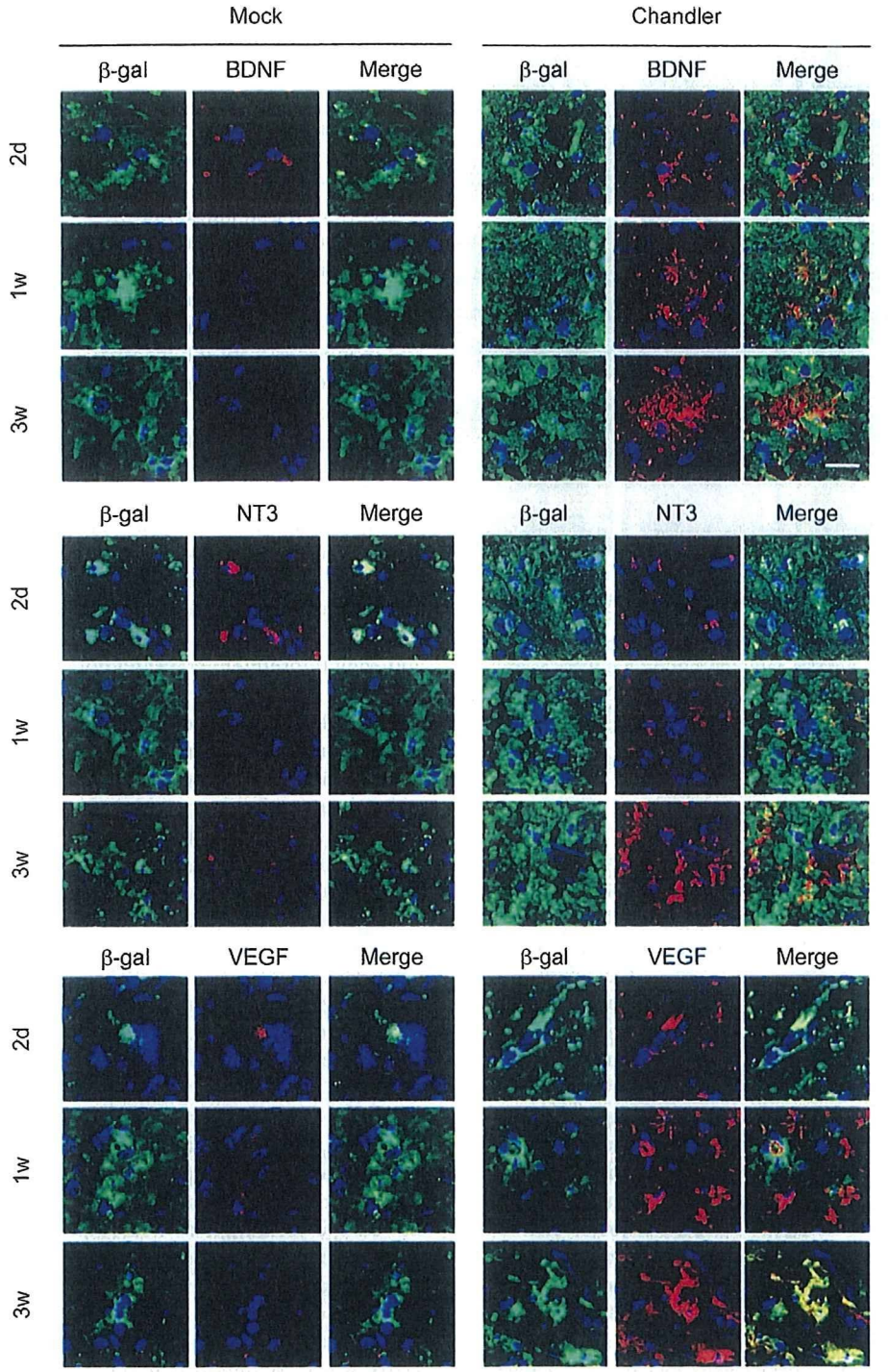

FIG. 5. Expression of trophic factors in hMSCs. hMSCs (1×10^5 cells) were transplanted into the left thalami of mice infected with strain Chandler and into those of mock-infected mice at 120 dpi. Two days (2d), 1 week (1w), and 3 weeks (3w) posttransplantation, cryosections were prepared and doubly stained with an anti-β-Gal MAb, for hMSCs (green), and an antibody against a human trophic factor (BDNF, NT3, or VEGF) (red). Nuclei were counterstained with DAPI (blue). Bar, 20 μm.

a beneficial effect without any adverse effects. How the introduction of MSCs leads to improved outcomes is not yet clear. However, the transplanted MSCs are known to migrate and home to a site of injury. Moreover, in this context, MSCs are expected to restore injured tissues by protecting neural tissues via secretion of various trophic factors (8), promotion of angiogenesis (20), stimulation of the proliferation and differentiation of endogenous neural stem cells (36), integration into tissues by differentiation or cell fusion (1), and modulation of the local immune response (64).

Here we showed that the level of migration of MSCs to the contralateral side of the mouse brain correlates with the de-

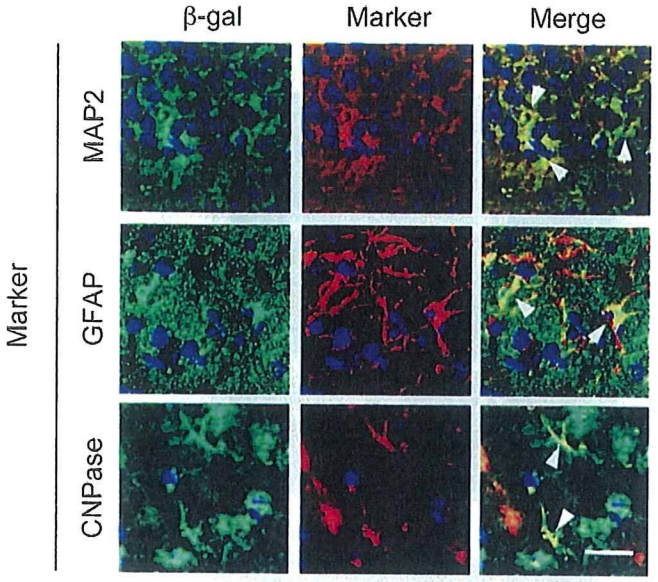

FIG. 6. Differentiation of hMSCs into cells of neuronal and glial lineages. At 120 dpi, hMSCs (1×10^5 cells) were transplanted into the left thalami of mice infected with strain Chandler. Three weeks post-transplantation, cryosections were prepared and doubly stained with an anti-β-Gal MAb, for hMSCs (green), and an antibody against a marker for neurons (MAP2), astrocytes (GFAP), or oligodendrocytes (CNPase) (red). Nuclei were counterstained with DAPI (blue). Arrows indicate hMSCs positive for each marker protein. The brain region for MAP2 and GFAP is the ipsilateral hippocampus, while that for CNPase is the cerebral cortex. Bar, 20 μm.

gree of PrP^{Sc} accumulation and the severity of histopathological changes in the prion-infected brain (Fig. 1d and 2). Although no antigen-specific humoral or cellular immune response is provoked in prion diseases, microglial activation and astrocytosis are prominent features of the diseases. Indeed, the expression of inflammatory cytokines and chemokines, which are likely to be produced in glial cells, is upregulated in the middle to late stage of prion infection (5, 6). In addition, brain extracts from prion-infected mice promoted chemotaxis of hMSCs in vitro. These results suggest that certain factors produced in the brains of prion-infected mice act as chemoattractive factors for hMSCs, although it is not clear whether the effects of mouse factors on human MSCs are as efficient as those on homologous MSCs. Monocyte chemoattractive protein 1 (known as CCL2), interleukin-8 (IL-8), and macrophage inflammatory protein 1α (known as CCL3) have been reported to enhance the migration of MSCs to ischemic brain tissue (57, 58). It was recently reported that an interaction between stromal cell-derived factor 1 (known as CXCL12), produced in ischemic brain lesions, and CXCR4, expressed on MSCs, plays an important role in the migration of MSCs (59). Because the inflammatory response and glial activation are common events in many neurological disorders, it is conceivable that a similar mechanism may account to some extent for the migration of MSCs to brain lesions associated with prion disease. For instance, we have found that the expression of CCL3 is upregulated in the thalami and medullae of prion-infected mice (unpublished observation). Experiments are under way to identify the chemoattractive factors by use of an in vitro chemotaxis assay.

MSCs have been reported to migrate to a site of brain injury even when intravenously injected (37, 38). Consistent with previous reports, our results showed here that hMSCs transplanted via intravenous injection travel to areas of brain lesions in prion-infected mice (Fig. 3). In prion diseases, although impairment of the blood-brain barrier (BBB) was observed in the cerebellum (56), no significant impairment of the BBB was observed in the hippocampus or cerebral cortex at the time of clinical onset or even at a later stage (42, 56). Thus, passive translocation of MSCs to the brain parenchyma through a disrupted BBB seems unlikely. Instead, active transendothelial migration of MSCs, similar to the recruitment of leukocytes and monocytes from the bloodstream to an inflammation site, is expected to be involved in the engraftment of MSCs transplanted via intravenous injection. Vascular cell adhesion molecule 1 and p-selectin expressed on the endothelium are important for the adhesion of MSCs to the endothelium via the β1 integrin VLA-4 (16, 46, 51). Proinflammatory cytokines, such as tumor necrosis factor alpha and IL-1β, upregulate the expression of adhesion molecules in endothelial cells (32). Indeed, tumor necrosis factor alpha and IL-1β are upregulated during the course of prion disease (6, 49), suggesting that these cytokines induce the adherence of MSCs to the endothelium and their subsequent transendothelial migration to the brain lesions. Understanding how the migration of MSCs to brain lesions affected by prion diseases is regulated, and further elucidation of the mechanisms underlying the tropism of MSCs, may provide new insight into the engraftment of MSCs as it relates to the progression and possible treatment of neurodegenerative diseases.

The ability of MSCs to migrate to a site of injury has been given particular attention, because it suggests that these cells can act as a vehicle for gene therapy in addition to aiding in the regeneration of degenerated tissues. Indeed, MSCs expressing genes of therapeutic potential showed a greater positive effect on functional recovery than unmodified MSCs (24, 37, 38). Transgenic expression of anti-PrP antibodies (22), a fusion protein between PrP^C and the Fc portion of immunoglobulin (PrP-Fc) (34), and dominant-negative PrP mutants (40) inhibited prion propagation. In addition, expression of anti-PrP Fab fragments and PrP-Fc in the brain by virus vectors has been reported to antagonize prion propagation in the brain (18, 62). Furthermore, intraventricular infusion of an anti-PrP MAb slowed the formation of neuropathological lesions and prolonged the survival of prion-infected mice even when the MAb was administered at clinical onset (53). However, large macromolecules, such as immunoglobulins, are expected to be delivered to the lesions inefficiently. Indeed, the distribution of MAbs was restricted primarily to the hippocampus and thalamus, even when the MAbs were infused directly into the lateral ventricle (53). Therefore, the observation that hMSCs target and home to brain lesions associated with prion diseases indicates the potential utility of hMSCs as a cellular vehicle for the delivery of therapeutic genes to brain lesions.

We showed here that microenvironments in the brain lesions associated with prion disease stimulate MSCs to produce various trophic factors: BDNF, NGF, VEGF, and others. These trophic factors are reported to have antiapoptotic effects, to promote nerve fiber regeneration, and to induce endogenous cell proliferation and angiogenesis in injured brains (9, 29, 31).

It remains to be elucidated whether the prolonged survival of prion-infected mice by hMSC transplantation can be attributed to the secretion of trophic factors from hMSCs. Although hMSCs alone may have the ameliorative effect to some extent, they could not arrest the disease progression caused by prion propagation. Similarly, it has been shown that antagonizing prion propagation can slow disease progression but cannot ameliorate functional deficits (13, 25, 53). Thus, it seems possible that the combination of MSCs with inhibitors of prion propagation would have a synergistic effect in the treatment of prion diseases.

Replacement of damaged neurons with differentiated MSCs or their fusion with MSCs after MSC transplantation is an attractive possible route to the restoration of neurological functions (11, 54, 60). In this study, we showed that small populations of MSCs were differentiated into cells expressing neuronal, astrocyte, or oligodendrocyte markers. Because only a small portion of transplanted MSCs differentiated into a neuronal and a glial lineage in vivo, it seems unlikely that the prolongation of survival could be attributed directly to differentiation. However, induction of neuronal differentiation in vitro prior to transplantation improves functional outcomes in a rat model of Parkinson's disease and cerebral infarction (12, 35). Therefore, appropriate preconditioning may enhance the effects of *trans*-differentiation on the restoration of degenerated tissues.

To our knowledge, this is the first report showing the therapeutic potential of MSCs for prion diseases. We showed that hMSCs home to the lesions, produce trophic factors, and differentiate into neuronal and glial lineage cells in response to the microenvironment in the lesions. As we are already aware, not only inhibition of prion propagation but also regeneration of damaged nervous tissues is required for recovery from prion diseases. Thus, a combination of genes possessing antiprion effects with MSCs, which can deliver therapeutic genes and have potential for neuroprotection and the regeneration of damaged tissues, may provide an effective treatment for prion diseases.

ACKNOWLEDGMENTS

This work was supported by the Regional New Consortium R&D Projects of the Ministry of Economy, Trade and Industry of Japan; by a grant from the global COE Program (F-001), a Grant-in-Aid for Science Research (A) (grant 18208026), and a Grant-in-Aid for Exploratory Research (grant 20658070) from the Ministry of Education, Culture, Sports, Science, and Technology of Japan; and by a grant from the Ministry of Health, Labor and Welfare of Japan (grant 20330701). This work was also partly supported by a grant for Strategic Cooperation to Control Emerging and Reemerging Infections and by the Program of Founding Research Centers for Emerging and Reemerging Infectious Diseases, from the Ministry of Education, Culture, Sports, Science, and Technology of Japan.

REFERENCES

1. **Alvarez-Dolado, M., R. Pardal, J. M. Garcia-Verdugo, J. R. Fike, H. O. Lee, K. Pfeffer, C. Lois, S. J. Morrison, and A. Alvarez-Buylla.** 2003. Fusion of bone-marrow-derived cells with Purkinje neurons, cardiomyocytes and hepatocytes. Nature **425**:968–973.
2. **Azizi, S. A., D. Stokes, B. J. Augelli, C. DiGirolamo, and D. J. Prockop.** 1998. Engraftment and migration of human bone marrow stromal cells implanted in the brains of albino rats—similarities to astrocyte grafts. Proc. Natl. Acad. Sci. USA **95**:3908–3913.
3. **Bang, O. Y., J. S. Lee, P. H. Lee, and G. Lee.** 2005. Autologous mesenchymal stem cell transplantation in stroke patients. Ann. Neurol. **57**:874–882.
4. **Bone, I., L. Belton, A. S. Walker, and J. Darbyshire.** 2008. Intraventricular pentosan polysulphate in human prion diseases: an observational study in the UK. Eur. J. Neurol. **15**:458–464.
5. **Burwinkel, M., C. Riemer, A. Schwarz, J. Schultz, S. Neidhold, T. Bamme, and M. Baier.** 2004. Role of cytokines and chemokines in prion infections of the central nervous system. Int. J. Dev. Neurosci. **22**:497–505.
6. **Campbell, I. L., M. Eddleston, P. Kemper, M. B. Oldstone, and M. V. Hobbs.** 1994. Activation of cerebral cytokine gene expression and its correlation with onset of reactive astrocyte and acute-phase response gene expression in scrapie. J. Virol. **68**:2383–2387.
7. **Chen, J., Y. Li, L. Wang, M. Lu, X. Zhang, and M. Chopp.** 2001. Therapeutic benefit of intracerebral transplantation of bone marrow stromal cells after cerebral ischemia in rats. J. Neurol. Sci. **189**:49–57.
8. **Chopp, M., and Y. Li.** 2002. Treatment of neural injury with marrow stromal cells. Lancet Neurol. **1**:92–100.
9. **Crigler, L., R. C. Robey, A. Asawachaicharn, D. Gaupp, and D. G. Phinney.** 2006. Human mesenchymal stem cell subpopulations express a variety of neuro-regulatory molecules and promote neuronal cell survival and neuritogenesis. Exp. Neurol. **198**:54–64.
10. **Demaimay, R., K. T. Adjou, V. Beringue, S. Demart, C. I. Lasmézas, J. P. Deslys, M. Seman, and D. Dormont.** 1997. Late treatment with polyene antibiotics can prolong the survival time of scrapie-infected animals. J. Virol. **71**:9685–9689.
11. **Deng, J., B. E. Petersen, D. A. Steindler, M. L. Jorgensen, and E. D. Laywell.** 2006. Mesenchymal stem cells spontaneously express neural proteins in culture and are neurogenic after transplantation. Stem Cells **24**:1054–1064.
12. **Dezawa, M., H. Kanno, M. Hoshino, H. Cho, N. Matsumoto, Y. Itokazu, N. Tajima, H. Yamada, H. Sawada, H. Ishikawa, T. Mimura, M. Kitada, Y. Suzuki, and C. Ide.** 2004. Specific induction of neuronal cells from bone marrow stromal cells and application for autologous transplantation. J. Clin. Investig. **113**:1701–1710.
13. **Doh-ura, K., K. Ishikawa, I. Murakami-Kubo, K. Sasaki, S. Mohri, R. Race, and T. Iwaki.** 2004. Treatment of transmissible spongiform encephalopathy by intraventricular drug infusion in animal models. J. Virol. **78**:4999–5006.
14. **Farquhar, C. F., and A. G. Dickinson.** 1986. Prolongation of scrapie incubation period by an injection of dextran sulphate 500 within the month before or after infection. J. Gen. Virol. **67**:463–473.
15. **Ferrari, G., G. Cusella-De Angelis, M. Coletta, E. Paolucci, A. Stornaiuolo, G. Cossu, and F. Mavilio.** 1998. Muscle regeneration by bone marrow-derived myogenic progenitors. Science **279**:1528–1530.
16. **Fox, J. M., G. Chamberlain, B. A. Ashton, and J. Middleton.** 2007. Recent advances into the understanding of mesenchymal stem cell trafficking. Br. J. Haematol. **137**:491–502.
17. **Furuoka, H., A. Yabuzoe, M. Horiuchi, Y. Tagawa, T. Yokoyama, Y. Yamakawa, M. Shinagawa, and T. Sata.** 2005. Effective antigen-retrieval method for immunohistochemical detection of abnormal isoform of prion proteins in animals. Acta Neuropathol. **109**:263–271.
18. **Genoud, N., D. Ott, N. Braun, M. Prinz, P. Schwarz, U. Suter, D. Trono, and A. Aguzzi.** 2008. Antiprion prophylaxis by gene transfer of a soluble prion antagonist. Am. J. Pathol. **172**:1287–1296.
19. **Goñi, F., E. Knudsen, F. Schreiber, H. Scholtzova, J. Pankiewicz, R. Carp, H. C. Meeker, R. Rubenstein, D. R. Brown, M. S. Sy, J. A. Chabalgoity, E. M. Sigurdsson, and T. Wisniewski.** 2005. Mucosal vaccination delays or prevents prion infection via an oral route. Neuroscience **133**:413–421.
20. **Hamano, K., T. S. Li, T. Kobayashi, S. Kobayashi, M. Matsuzaki, and K. Esato.** 2000. Angiogenesis induced by the implantation of self-bone marrow cells: a new material for therapeutic angiogenesis. Cell Transplant. **9**:439–443.
21. **Hellmann, M. A., H. Panet, Y. Barhum, E. Melamed, and D. Offen.** 2006. Increased survival and migration of engrafted mesenchymal bone marrow stem cells in 6-hydroxydopamine-lesioned rodents. Neurosci. Lett. **395**:124–128.
22. **Heppner, F. L., C. Musahl, I. Arrighi, M. A. Klein, T. Rülicke, B. Oesch, R. M. Zinkernagel, U. Kalinke, and A. Aguzzi.** 2001. Prevention of scrapie pathogenesis by transgenic expression of anti-prion protein antibodies. Science **294**:178–182.
23. **Hofstetter, C. P., E. J. Schwarz, D. Hess, J. Widenfalk, A. El Manira, D. J. Prockop, and L. Olson.** 2002. Marrow stromal cells form guiding strands in the injured spinal cord and promote recovery. Proc. Natl. Acad. Sci. USA **99**:2199–2204.
24. **Jin, H. K., J. E. Carter, G. W. Huntley, and E. H. Schuchman.** 2002. Intracerebral transplantation of mesenchymal stem cells into acid sphingomyelinase-deficient mice delays the onset of neurological abnormalities and extends their life span. J. Clin. Investig. **109**:1183–1191.
25. **Kawasaki, Y., K. Kawagoe, C. J. Chen, K. Teruya, Y. Sakasegawa, and K. Doh-ura.** 2007. Orally administered amyloidophilic compound is effective in prolonging the incubation periods of animals cerebrally infected with prion diseases in a prion strain-dependent manner. J. Virol. **81**:12889–12898.
26. **Kobune, M., Y. Kawano, Y. Ito, H. Chiba, K. Nakamura, H. Tsuda, K. Sasaki, H. Dehari, H. Uchida, O. Honmou, S. Takahashi, A. Bizen, R. Takimoto, T. Matsunaga, J. Kato, K. Kato, K. Houkin, Y. Niitsu, and H. Hamada.** 2003. Telomerized human multipotent mesenchymal cells can dif-

ferentiate into hematopoietic and cobblestone area-supporting cells. Exp. Hematol. 31:715–722.
27. **Kocisko, D. A., W. S. Caughey, R. E. Race, G. Roper, B. Caughey, and J. D. Morrey.** 2006. A porphyrin increases survival time of mice after intracerebral prion infection. Antimicrob. Agents Chemother. 50:759–761.
28. **Lee, P. H., J. W. Kim, O. Y. Bang, Y. H. Ahn, I. S. Joo, and K. Huh.** 2008. Autologous mesenchymal stem cell therapy delays the progression of neurological deficits in patients with multiple system atrophy. Clin. Pharmacol. Ther. 83:723–730.
29. **Li, Y., J. Chen, X. G. Chen, L. Wang, S. C. Gautam, Y. X. Xu, M. Katakowski, L. J. Zhang, M. Lu, N. Janakiraman, and M. Chopp.** 2002. Human marrow stromal cell therapy for stroke in rat: neurotrophins and functional recovery. Neurology 59:514–523.
30. **Li, Y., J. Chen, L. Wang, L. Zhang, M. Lu, and M. Chopp.** 2001. Intracerebral transplantation of bone marrow stromal cells in a 1-methyl-4-phenyl-1,2,3,6-tetrahydropyridine mouse model of Parkinson's disease. Neurosci. Lett. 316:67–70.
31. **Mahmood, A., D. Lu, and M. Chopp.** 2004. Marrow stromal cell transplantation after traumatic brain injury promotes cellular proliferation within the brain. Neurosurgery 55:1185–1193.
32. **Mantovani, A., F. Bussolino, and E. Dejana.** 1992. Cytokine regulation of endothelial cell function. FASEB J. 6:2591–2599.
33. **Mazzini, L., K. Mareschi, I. Ferrero, E. Vassallo, G. Oliveri, N. Nasuelli, G. D. Oggioni, L. Testa, and F. Fagioli.** 2008. Stem cell treatment in amyotrophic lateral sclerosis. J. Neurol. Sci. 265:78–83.
34. **Meier, P., N. Genoud, M. Prinz, M. Maissen, T. Rülicke, A. Zurbriggen, A. J. Raeber, and A. Aguzzi.** 2003. Soluble dimeric prion protein binds PrP^{Sc} *in vivo* and antagonizes prion disease. Cell 113:49–60.
35. **Mimura, T., M. Dezawa, H. Kanno, and I. Yamamoto.** 2005. Behavioral and histological evaluation of a focal cerebral infarction rat model transplanted with neurons induced from bone marrow stromal cells. J. Neuropathol. Exp. Neurol. 64:1108–1117.
36. **Munoz, J. R., B. R. Stoutenger, A. P. Robinson, J. L. Spees, and D. J. Prockop.** 2005. Human stem/progenitor cells from bone marrow promote neurogenesis of endogenous neural stem cells in the hippocampus of mice. Proc. Natl. Acad. Sci. USA 102:18171–18176.
37. **Nakamura, K., Y. Ito, Y. Kawano, K. Kurozumi, M. Kobune, H. Tsuda, A. Bizen, O. Honmou, Y. Niitsu, and H. Hamada.** 2004. Antitumor effect of genetically engineered mesenchymal stem cells in a rat glioma model. Gene Ther. 11:1155–1164.
38. **Nomura, T., O. Honmou, K. Harada, K. Houkin, H. Hamada, and J. D. Kocsis.** 2005. I.V. infusion of brain-derived neurotrophic factor gene-modified human mesenchymal stem cells protects against injury in a cerebral ischemia model in adult rat. Neuroscience 136:161–169.
39. **Paxinos, G., and K. B. J. Franklin.** 2001. The mouse brain in stereotaxic coordinates. Academic Press, Inc., San Diego, CA.
40. **Perrier, V., K. Kaneko, J. Safar, J. Vergara, P. Tremblay, S. J. DeArmond, F. E. Cohen, S. B. Prusiner, and A. C. Wallace.** 2002. Dominant-negative inhibition of prion replication in transgenic mice. Proc. Natl. Acad. Sci. USA 99:13079–13084.
41. **Pittenger, M. F., A. M. Mackay, S. C. Beck, R. K. Jaiswal, R. Douglas, J. D. Mosca, M. A. Moorman, D. W. Simonetti, S. Craig, and D. R. Marshak.** 1999. Multilineage potential of adult human mesenchymal stem cells. Science 284:143–147.
42. **Priller, J., M. Prinz, M. Heikenwalder, N. Zeller, P. Schwarz, F. L. Heppner, and A. Aguzzi.** 2006. Early and rapid engraftment of bone marrow-derived microglia in scrapie. J. Neurosci. 26:11753–11762.
43. **Priola, S. A., A. Raines, and W. S. Caughey.** 2000. Porphyrin and phthalocyanine antiscrapie compounds. Science 287:1503–1506.
44. **Prockop, D. J.** 1997. Marrow stromal cells as stem cells for nonhematopoietic tissues. Science 276:71–74.
45. **Rainov, N. G., Y. Tsuboi, P. Krolak-Salmon, A. Vighetto, and K. Doh-Ura.** 2007. Experimental treatments for human transmissible spongiform encephalopathies: is there a role for pentosan polysulfate? Expert Opin. Biol. Ther. 7:713–726.
46. **Rüster, B., S. Göttig, R. J. Ludwig, R. Bistrian, S. Müller, E. Seifried, J. Gille, and R. Henschler.** 2006. Mesenchymal stem cells display coordinated rolling and adhesion behavior on endothelial cells. Blood 108:3938–3944.
47. **Ryan, J. M., F. P. Barry, J. M. Murphy, and B. P. Mahon.** 2005. Mesenchymal stem cells avoid allogeneic rejection. J. Inflamm. 2:8.
48. **Sanchez-Ramos, J. R.** 2002. Neural cells derived from adult bone marrow and umbilical cord blood. J. Neurosci. Res. 69:880–893.
49. **Schultz, J., A. Schwarz, S. Neidhold, M. Burwinkel, C. Riemer, D. Simon, M. Kopf, M. Otto, and M. Baier.** 2004. Role of interleukin-1 in prion disease-associated astrocyte activation. Am. J. Pathol. 165:671–678.
50. **Schwarz, A., O. Krätke, M. Burwinkel, C. Riemer, J. Schultz, P. Henklein, T. Bamme, and M. Baier.** 2003. Immunisation with a synthetic prion protein-derived peptide prolongs survival times of mice orally exposed to the scrapie agent. Neurosci. Lett. 350:187–189.
51. **Segers, V. F., I. Van Riet, L. J. Andries, K. Lemmens, M. J. Demolder, A. J. De Becker, M. M. Kockx, and G. W. De Keulenaer.** 2006. Mesenchymal stem cell adhesion to cardiac microvascular endothelium: activators and mechanisms. Am. J. Physiol. Heart Circ. Physiol. 290:H1370–H1377.
52. **Sigurdsson, E. M., D. R. Brown, M. Daniels, R. J. Kascsak, R. Kascsak, R. Carp, H. C. Meeker, B. Frangione, and T. Wisniewski.** 2002. Immunization delays the onset of prion disease in mice. Am. J. Pathol. 161:13–17.
53. **Song, C. H., H. Furuoka, C. L. Kim, M. Ogino, A. Suzuki, R. Hasebe, and M. Horiuchi.** 2008. Effect of intraventricular infusion of anti-prion protein monoclonal antibodies on disease progression in prion-infected mice. J. Gen. Virol. 89:1533–1544.
54. **Terada, N., T. Hamazaki, M. Oka, M. Hoki, D. M. Mastalerz, Y. Nakano, E. M. Meyer, L. Morel, B. E. Petersen, and E. W. Scott.** 2002. Bone marrow cells adopt the phenotype of other cells by spontaneous cell fusion. Nature 416:542–545.
55. **Trevitt, C. R., and J. Collinge.** 2006. A systematic review of prion therapeutics in experimental models. Brain 129:2241–2265.
56. **Vorbrodt, A. W., D. H. Dobrogowska, M. Tarnawski, H. C. Meeker, and R. I. Carp.** 1997. Immunocytochemical evaluation of blood-brain barrier to endogenous albumin in scrapie-infected mice. Acta Neuropathol. 93:341–348.
57. **Wang, L., Y. Li, J. Chen, S. C. Gautam, Z. Zhang, M. Lu, and M. Chopp.** 2002. Ischemic cerebral tissue and MCP-1 enhance rat bone marrow stromal cell migration in interface culture. Exp. Hematol. 30:831–836.
58. **Wang, L., Y. Li, X. Chen, J. Chen, S. C. Gautam, Y. Xu, and M. Chopp.** 2002. MCP-1, MIP-1, IL-8 and ischemic cerebral tissue enhance human bone marrow stromal cell migration in interface culture. Hematology 7:113–117.
59. **Wang, Y., Y. Deng, and G. Q. Zhou.** 2008. SDF-1α/CXCR4-mediated migration of systemically transplanted bone marrow stromal cells towards ischemic brain lesion in a rat model. Brain Res. 1195:104–112.
60. **Wislet-Gendebien, S., G. Hans, P. Leprince, J. M. Rigo, G. Moonen, and B. Rogister.** 2005. Plasticity of cultured mesenchymal stem cells: switch from nestin-positive to excitable neuron-like phenotype. Stem Cells 23:392–402.
61. **Woodbury, D., E. J. Schwarz, D. J. Prockop, and I. B. Black.** 2000. Adult rat and human bone marrow stromal cells differentiate into neurons. J. Neurosci. Res. 61:364–370.
62. **Wuertzer, C. A., M. A. Sullivan, X. Qiu, and H. J. Federoff.** 2008. CNS delivery of vectored prion-specific single-chain antibodies delays disease onset. Mol. Ther. 16:481–486.
63. **Yamaguchi, S., H. Wakimoto, Y. Yoshida, Y. Kanegae, I. Saito, M. Aoyagi, K. Hirakawa, T. Amagasa, and H. Hamada.** 1995. Enhancement of retrovirus-mediated gene transduction efficiency by transient overexpression of the amphotropic receptor, GLVR-2. Nucleic Acids Res. 23:2080–2081.
64. **Zappia, E., S. Casazza, E. Pedemonte, F. Benvenuto, I. Bonanni, E. Gerdoni, D. Giunti, A. Ceravolo, F. Cazzanti, F. Frassoni, G. Mancardi, and A. Uccelli.** 2005. Mesenchymal stem cells ameliorate experimental autoimmune encephalomyelitis inducing T-cell anergy. Blood 106:1755–1761.

Virology 394 (2009) 200–207

Contents lists available at ScienceDirect

Virology

journal homepage: www.elsevier.com/locate/yviro

Generation of monoclonal antibody that distinguishes PrP^{Sc} from PrP^{C} and neutralizes prion infectivity

Motohiro Horiuchi [a,*], Ayako Karino [b], Hidefumi Furuoka [c], Naotaka Ishiguro [d], Kumiko Kimura [e], Morikazu Shinagawa [f]

[a] Laboratory of Prion Diseases, Graduate School of Veterinary Medicine, Hokkaido University, Kita-18, Nishi-9, Kita-ku, Sapporo, Hokkadio 060-0818, Japan
[b] Department of Veterinary Public Health, Obihiro University of Agriculture and Veterinary Medicine, Inada-cho, Obihiro, Hokkaido 080-8555, Japan
[c] Department of Pathological Science, Obihiro University of Agriculture and Veterinary Medicine, Inada-cho, Obihiro, Hokkaido 080-8555, Japan
[d] Laboratory of Food and Environmental Hygiene, Faculty of Applied Biological Science, Gifu University, Yanagito, Gifu 501-1193, Japan
[e] Bovine Pathology Unit, National Institute of Animal Health, Kannondai, Tsukuba, Ibaraki 305-0856, Japan
[f] Prion Disease Research Center, National Institute of Animal Health, Kannondai, Tsukuba, Ibaraki 305-0856, Japan

ARTICLE INFO

Article history:
Received 21 April 2009
Returned to author for revision 2 June 2009
Accepted 18 August 2009
Available online 18 September 2009

Keywords:
Prion
Transmissible spongiform encephalopathy
Monoclonal antibody
Peptide phage display
Infectivity

ABSTRACT

To establish PrP^{Sc}-specific mAbs, we immunized *Prnp*$^{-/-}$ mice with PrP^{Sc} purified from prion-infected mice. Using this approach, we obtained mAb 6H10, which reacted with PrP^{Sc} treated with proteinase K, but not with PrP^{Sc} pretreated with more than 3 M GdnHCl. In contrast, reactivity of pan-PrP mAbs increased with increasing concentrations of GdnHCl used for pretreatment of PrP^{Sc}. In histoblot analysis, mAb 6H10 showed a positive reaction on a non-denatured histoblot but reactivity was lower when the histoblot was pretreated by autoclaving. Epitope analysis suggested that the extreme C-terminus of PrP is likely to be part of the epitope for mAb 6H10. MAb 6H10 immunoprecipitated PrP^{Sc} from brains of mice, sheep, and cattle infected with prions. Furthermore, pretreatment of purified PrP^{Sc} with mAb 6H10 reduced the infectious titer more than 1 log. Taken together, these results suggest that mAb 6H10 recognizes a conformational epitope on PrP^{Sc} that is related to prion infectivity.

© 2009 Elsevier Inc. All rights reserved.

Introduction

Prion diseases are fatal neurodegenerative diseases which include scrapie in sheep and goats, bovine spongiform encephalopathy (BSE), and Creutzfeldt-Jakob diseases (CJD) in humans. A hallmark of the diseases is the accumulation of a pathogenic, abnormal isoform of prion protein, designated PrP^{Sc}, in the central nervous system of affected animals. PrP^{Sc} is generated from the host-encoded, cellular prion protein, PrP^{C}, by certain post-translational modification including conformational transformation (Prusiner et al., 1998). Although the two isoforms are encoded by the host gene, *PrP*, they differ from each other biochemically and biophysically. For example, PrP^{C} is soluble in non-ionic detergents and sensitive to protease treatment, whereas PrP^{Sc} is insoluble due to its propensity to form aggregates that are partially resistant to protease treatment (Oesch et al., 1985; Meyer et al., 1986). PrP^{C} has a high α-helix but low β-sheet content, whereas PrP^{Sc} has a higher β-sheet content (Caughey et al., 1991; Pan et al., 1993; Safar et al., 1993). However, PrP^{Sc} is comprised of PK-sensitive and PK-resistant PrP^{Sc}, such that PrP^{Sc} cannot be distinguished from PrP^{C} simply using protease treatment (Bessen and Marsh, 1994; Safar et al., 1998, 2005; Silveira et al., 2005).

To date, there have been a number of reports on the production of monoclonal and polyclonal antibodies against PrP molecules. Most of these are pan-PrP antibodies that recognize either linear or discontinuous epitopes on PrP^{C} and react with PrP^{Sc} pretreated with denaturant (Kascsak et al., 1987; Serban et al., 1990; Williamson et al., 1996; Peretz et al., 1997; Kim et al., 2004a). Because of the co-existence of PrP^{C} and PrP^{Sc}, and the propensity of PrP^{Sc} to form aggregates, removal of PrP^{C} by protease treatment and subsequent denaturation are prerequisites for specific detection of PrP^{Sc} by pan-PrP antibodies. However, the ability to analyze the properties of PrP^{Sc} using pan-PrP antibodies is limited, as the biological and biochemical properties of PrP^{Sc} are affected by protease treatment and denaturation.

Molecular probes that specifically react to PrP^{Sc} and distinguish PrP^{Sc} from PrP^{C} can be a powerful tool for analysis of the entity of PrP^{Sc}. For instance, PrP^{C} will be act as a molecular probe for PrP^{Sc}, as PrP^{C} binds to PrP^{Sc} (Horiuchi et al., 1999). A fusion protein comprised of PrP^{C} and the immunoglobulin Fc region and a genetically modified antibody possessing PrP^{C} segments have been demonstrated to bind to PrP^{Sc} possibly via the PrP^{C} segments (Meier et al., 2003; Moroncini et al., 2004). Moreover, plasminogen binds to PrP^{Sc} not to PrP^{C}; however, plasminogen will bind to other serum proteins and thus, selectivity of the binding is obscure (Fischer et al., 2000). In contrast to many reports of pan-PrP mAbs, only a few studies have reported anti-PrP^{Sc} antibodies that specifically discriminate PrP^{Sc} from PrP^{C} (Korth

* Corresponding author. Fax: +81 11 706 5293.
E-mail address: horiuchi@vetmed.hokudai.ac.jp (M. Horiuchi).

0042-6822/$ – see front matter © 2009 Elsevier Inc. All rights reserved.
doi:10.1016/j.virol.2009.08.025

et al., 1997; Paramithiotis et al., 2003; Curin Serbec et al., 2004; Jones et al., 2009).

Availability of a panel of PrP^{Sc}-specific antibodies is indispensable for analysis of the biochemical properties of PrP^{Sc}. Thus, in order to obtain PrP^{Sc}-specific antibodies, we immunized PrP-ablated (*Prnp*$^{-/-}$) mice with PrP^{Sc} purified from prion-infected mouse brains. Prion infectivity is thought to be associated with PrP^{Sc} oligomers; thus, we used non-denatured, purified PrP^{Sc} as the immunogen. One of the mAbs, clone 6H10, showed interesting reactivity to PrP molecules; mAb 6H10 reacted with non-denatured PrP^{Sc} but not with recombinant mouse PrP (rMoPrP) or denatured PrP^{Sc} in an enzyme-linked immunosorbent assay. This pattern of reactivity implied that mAb 6H10 recognizes PrP^{Sc} but not PrP^{C}, allowing for detailed characterization of mAb 6H10.

Results

Reactivity of mAb 6H10 to purified PrP^{Sc}

To obtain PrP^{Sc}-specific mAbs, we immunized *Prnp*$^{-/-}$ mice with a purified PrP^{Sc} fraction and hybridoma supernatants were screened with the purified PrP^{Sc} and rMoPrP by enzyme-linked immunosorbent assay (ELISA). We established one mAb, 6H10 (isotype: IgG2b), which reacted with purified PrP^{Sc} but not with rMoPrP or PrP^{Sc} denatured with 6 M GdnHCl. This pattern of reactivity suggests that mAb 6H10 might specifically recognize the PrP^{Sc} conformation and thus, we further analyzed mAb 6H10.

Figure 1 shows reactivity of mAb 6H10 and pan-PrP mAbs to purified PrP^{Sc}. The mAbs 31C6, 44B1, and 72, which were characterized as pan-PrP mAbs, reacted with purified PrP^{Sc} before proteinase K (PK) treatment (0 μg/ml), but reactivity disappeared when PrP^{Sc} was pretreated with 20 μg/ml or higher concentrations of PK (Fig. 1a). It is known that PrP^{Sc} forms sedimentable aggregates, and PrP^{C} or protease-sensitive PrP molecules, which are expected to expose the epitopes for pan-PrP mAbs, are usually co-purified with PrP^{Sc} during purification. Thus, the drastic decline in reactivity of pan-PrP mAbs with increases in PK concentration is probably due to removal of protease-sensitive PrP species from the purified PrP^{Sc} fraction. In contrast to the results of pan-PrP mAbs, mAb 6H10 reacted with PrP^{Sc} treated with up to 320 μg/ml of PK (Fig. 1a).

Most of epitopes for pan-PrP mAbs are buried in aggregates of purified PrP^{Sc}, and become exposed as denaturation reveals cryptic epitopes (Kim et al., 2004a). In contrast, PrP^{Sc}-specific conformational epitope(s), if they exist, would be expected to be destroyed upon denaturation. Consistent with this, reactivity of mAb 6H10 gradually decreased and disappeared when PK-treated PrP^{Sc} was treated with more than 3 M GdnHCl (Fig. 1b). This is different from pan-PrP mAbs, which did not react with PK-treated PrP^{Sc} without denaturation (at 0 M GdnHCl) but reactivity became apparent and increased as the GdnHCl concentration is increased (Fig. 1b). Taken together, the results suggested that mAb 6H10 recognizes a conformational epitope on PrP^{Sc}. Consistent with this, mAb 6H10 did not react with PrP^{Sc} in immunoblot analysis (Fig. 2a). To confirm reactivity of mAb 6H10 to PrP^{Sc}, we performed immunoprecipitation analysis. The mAb 6H10 precipitated PrP^{Sc} into the bead-bound fraction from a suspension of a purified PrP^{Sc} fraction, whereas most of PrP^{Sc} remained in the unbound fraction in the case of mAb 31C6 or a negative control mAb (Fig. 2b). Following immunoprecipitation of PrP^{Sc} by mAb 6H10, the amount of PrP^{Sc} that remained in the corresponding supernatant was decreased.

Immunoprecipitation of PrP^{Sc} from brain homogenates by mAb 6H10

Next we performed immunoprecipitation from brain homogenates. The mAb 31C6 immunoprecipitated bands corresponding to PrP^{C} from brain homogenates of uninfected mouse, whereas mAb

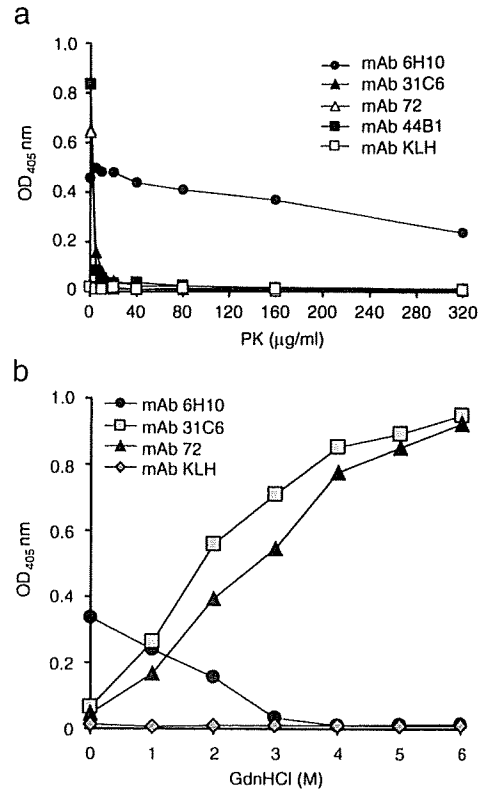

Fig. 1. Reactivity of mAb 6H10 to PrP^{Sc} in ELISA. (a) Reactivity to PK-treated PrP^{Sc}. Wells were coated with 200 ng/well of purified, PK-untreated PrP^{Sc} of the Obihiro strain. After adsorption, wells were treated with the indicated concentrations of PK. After terminating PK activity with Pefabloc, the wells were subjected to the antibody reaction. The anti-PrP mAbs used were 6H10, 31C6, 72, and 44B1. Anti-KLH mAb was used as a negative control mAb. (b) Effect of denaturation of PrP^{Sc}. Purified PrP^{Sc} adsorbed to the wells was digested with 20 μg/ml PK and treated with GdnHCl (0–6 M) at r.t. for 1 h. Then wells were subjected to the antibody reaction.

6H10 did not. PrP precipitated from brain homogenates of mice infected with the Obihiro or Chandler strain by mAb 31C6 disappeared after PK treatment. In contrast, 6–7 kDa smaller PrP bands were detected when fractions immunoprecipitated from brain

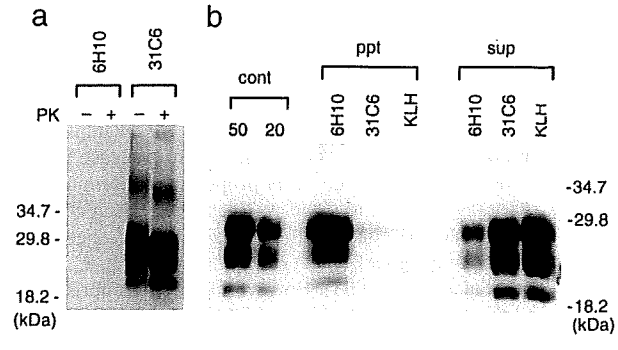

Fig. 2. Reactivity of mAb 6H10 to PrP^{Sc} in Immunoblotting. (a) Reactivity of mAbs 6H10 and 31C6 on an immunoblot. PK-treated (+) and PK-untreated (-) brain homogenates of mice infected with the Obihiro strain were subjected to immunoblotting. (b) Immunoprecipitation. PK-digested purified PrP^{Sc} of the Obihiro strain in PBS containing 1% Triton X-100 was incubated with antibodies as indicated at the top. The antigen-antibody complexes were collected with magnetic beads coated with protein G. PrP^{Sc} in precipitates (ppt) and supernatants (sup) were detected by immunoblotting using HRP-conjugated mAb 31C6. Anti-KLH mAb (KLH) was used as a negative control mAb. PK-digested PrP^{Sc} fractions at 50 and 20 μg brain equivalents were loaded as controls.

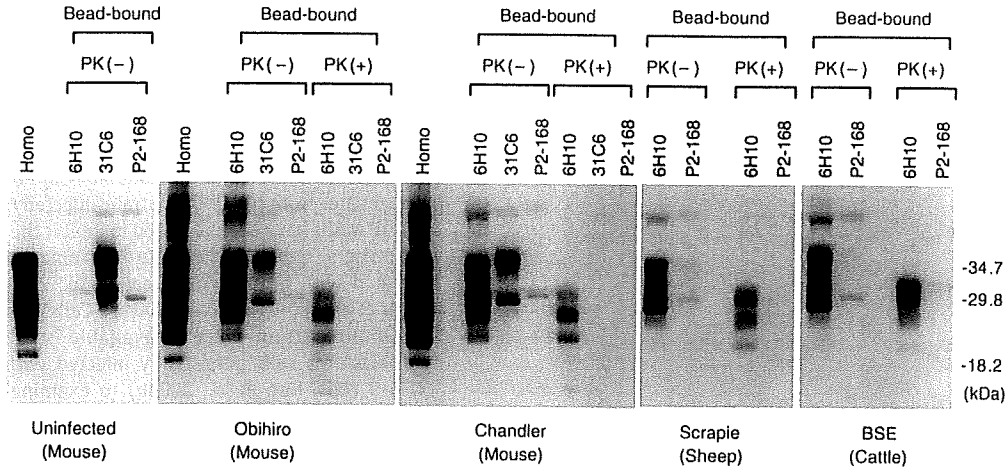

Fig. 3. Immunoprecipitation of PrP^{Sc} by mAb 6H10. Brain homogenates (2.5%) of prion-infected or uninfected animals were incubated with 10 μg of mAbs (6H10, 31C6, P2-168) and then immunoprecipitated with protein G coupled magnetic beads. Bead-bound fractions were treated with PK [PK(+)] or not [PK(-)] and then subjected to immunoblotting. The blots were probed with HRP-conjugated mAb 31C6. MAb P2-168 was used as a negative control mAb. Homo, brain homogenates of uninfected mice or mice infected with prions.

homogenates of the Obihiro or Chandler strain-infected mice with mAb 6H10 were treated with PK (Fig. 3). Thus, at least, some fraction of the PrP immunoprecipitated with mAb 6H10 was resistant to PK treatment. These results suggest that mAb 6H10 selectively recognizes an epitope specific to PrP^{Sc} and thus has a potential to distinguish PrP^{Sc} from PrP^{C}. Moreover, mAb 6H10 exhibited broad host specificity; the mAb reacted with PrP^{Sc} in the brains of scrapie-affected sheep and BSE-affected cattle (Fig. 3). These results suggest that, if not all, at least a certain population of PrP^{Sc} in the brains of prion-infected animals possesses the epitope for mAb 6H10 on its surface.

Recently, Biasini et al. (2008) reported that mAb 15B3, which is purported to be specific to PrP^{Sc} (Korth et al., 1997), also reacted with non-infectious PrP aggregates. Thus we analyzed reactivity of mAb 6H10 to PrP aggregates prepared from rMoPrP89-231 purified from *Escherichia coli* (Fig. 4). The mAb 31C6 immunoprecipitated both non-aggregated and aggregated rMoPrP89-231. In contrast, mAb 6H10 did not immunoprecipitate non-aggregated rMoPrP89-231, but showed weak reaction to aggregated rMoPrP89-231 at the same level as an isotype-matched negative control (mAb P2-168). Thus, the reaction of mAb 6H10 to aggregated rMoPrP89-231 appears to be a non-specific reaction that is possibly caused by a hydrophobic property of aggregated rMoPrP89-231. The same results were obtained when rMoPrP23-231 was used (data not shown). Considering that mAb P2-168 did not immunoprecipitate PrP^{Sc} from brains of prion-infected animals, again, the reactivity of mAb 6H10 to PrP^{Sc} in immunoprecipitation is thought to be a specific reaction between mAb 6H10 and the epitope on PrP^{Sc}.

Reactivity of mAb 6H10 to prion-infected and uninfected brain in histoblot

To further analyze the reactivity of mAb 6H10 to PrP^{Sc}, we performed histoblot analysis (Fig. 5a). Two pan-PrP anitbodies, one of which is antiserum of $Prnp^{-/-}$ mice immunized with rMoPrP (NIAH), and the other is mAb 110, showed positive reaction to histoblot of prion-infected and uninfected mouse brains. However, the positive signals nearly disappeared when the blots were pretreated with PK, indicating that the signals represented protease-sensitive PrP. When the PK-treated histoblots were further processed by autoclaving, which partially denatures PrP^{Sc} and thus exposes cryptic epitopes, these antibodies reacted only with prion-infected mouse brains. In contrast, mAb 6H10 reacted intensely to a histoblot of prion-infected mouse brain pretreated with PK and the intensity was drastically reduced by autoclaving of the histoblot. These results indicated that PrP^{Sc} accumulated in the brain possessed the epitope for mAb 6H10. Unexpectedly, mAb 6H10 showed weak reaction to PK-untreated, uninfected mouse brain sample, although the reaction was not observed on a PK-treated histoblot. To examine whether mAb 6H10 reacts not only with PrP^{Sc} but also PrP^{C} in a histoblot, we used brains of wild-type ($Prnp^{+/+}$) and $Prnp^{-/-}$ mice. The mAb 44B1, classified as pan-PrP mAb, reacted only with the brain of $Prnp^{+/+}$ mice as expected. However, mAb 6H10 reacted weakly with both $Prnp^{+/+}$ and $Prnp^{-/-}$ mice brains (Fig. 5b). Thus, the weak reaction of mAb 6H10 to the brains of uninfected mice may be the result of the presence of a host antigen(s) other than PrP^{C} that shares an epitope similar to that for mAb 6H10.

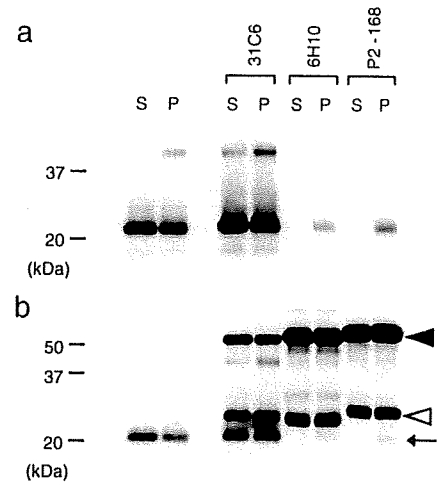

Fig. 4. Reactivity of mAb 6H10 to non-infectious PrP aggregates. (a) Immunoprecipitation of non-aggregated rMoPrP89-231 (S) and aggregated rMoPrP89-231 (P) with mAbs 31C6, 6H10, and P2-168. The mAb P2-168 is an isotype-matched negative control for mAb 6H10. Samples were prepared as described in Materials and Methods, and 10 μl of bead-bound fraction was loaded in each lane. The blot was probed with HRP-conjugated mAb 44B1. (b) After chemiluminescence reaction, the same blot in (a) was washed with PBST and re-probed with HRP-conjugated goat anti-mouse Igs (GE Healthcare) to ensure comparable amount of mAbs were used for each immunoprecipitation. Closed and open arrowhead indicate immunoglobulin heavy and light chain, respectively. Arrow indicates rMoPrP89-231 detected in the re-probing process.

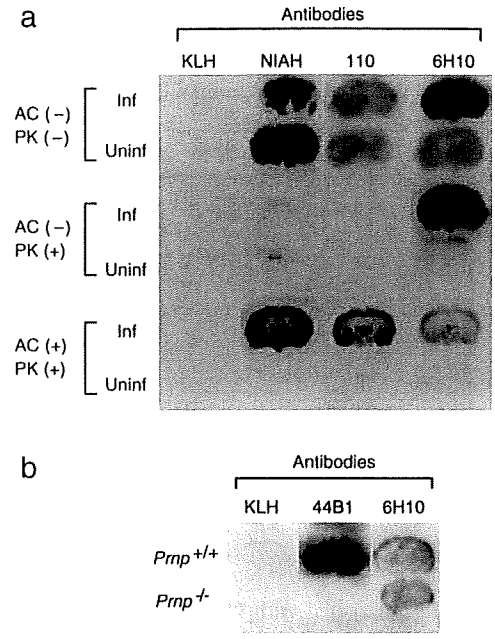

Fig. 5. Histoblot analysis. (a) Cryosections of Obihiro strain-infected (Inf) and uninfected mice brains (Uninf) were blotted onto PVDF membranes. The histoblots on the 1st row were neither treated with autoclave (AC-) nor PK (PK-). The blots on the 2nd row were treated with 50 μg/ml PK (PK+) but not with autoclave (AC-), and those on the 3rd row were treated with PK (PK+) and then autoclaved (AC+). Antibodies: KLH, negative control mAb; NIAH, serum of *Prnp*-/- mouse immunized with rMoPrP; 110, mAb 110; 6H10, mAb 6H10. (b) Histoblots of wild-type ($Prnp^{+/+}$) and $Prnp^{-/-}$ mouse brains were stained with antibodies as indicated.

Neutralization of prion infectivity by mAb 6H10

Next, we examined whether mAb 6H10 can neutralize prion infectivity. Purified PrP^{Sc} from mice infected with the Obihiro strain was pre-incubated with mAbs and then inoculated intracerebrally to mice for a bioassay (Table 1). Pre-incubation of PrP^{Sc} with mAb 6H10 prolonged the mean incubation time by 19 days compared to PrP^{Sc} pretreated with negative control mAbs anti-KLH ($p<0.01$), whereas pre-treatment with mAb 31C6 or 110 appeared to prolong the incubation time a little but the differences were not significant. A prolongation of 19 days was inferred as corresponding to a more than 95% reduction in prion infectivity based on the infectivity–incubation time standard curve obtained from bioassays of serially diluted brain homogenates from the Obihiro strain-infected mice (Table 1). Several pan-PrP mAbs have been reported to inhibit the accumulation of PrP^{Sc} in prion persistently infected neuroblastoma cells when the cells were incubated with those mAbs (Enari et al., 2001; Peretz et al., 2001; Perrier et al., 2004; Kim et al., 2004b). Cells persistently infected with the Obihiro strain were unavailable so far, we used mouse neuroblastoma cells persistently infected with the Chandler strain (I3/I5-9 cells, Kim et al., 2004b) to examine whether mAb 6H10 inhibits PrP^{Sc} formation in cells. Cells were cultured with mAb 6H10 (up to 20 μg/ml) for 4 days; however, mAb 6H10 did not affect the PrP^{Sc} formation in I3/I5-9 (data not shown). Our previous study showed that anti-PrP mAbs strongly reacted with PrP^{C} on the cell surface could inhibit PrP^{Sc} formation in I3/I5-9 cells (Kim et al., 2004b). However, mAb 6H10 did not react with cell surface of I3/I5-9 cells by flowcytometirc analysis (data not shown).

Table 1
Neutralization of prion infectivity by mAb 6H10.

mAb	Numbers of mice		Incubation time to terminal stage [mean ± SD (days)]
	Inoculated	PrP^{Sc} positive	
Anti-KLH	5	5	161 ± 4
mAb 31C6	5	5	166 ± 6
mAb 110	5	5	169 ± 7
mAb 6H10	5	5	180 ± 8[a]
Brain homogenate[b]			
10%	10	10	161 ± 6
1%	12	12	164 ± 6
0.1%	12	12	175 ± 6
0.01%	11	11	189 ± 18
0.001%	12	12	212 ± 12
0.0001%	11	11	245 ± 31
0.00001%	6	3	278 ± 52
0.000001%	6	0	>393

[a] $p<0.01$ by ANOVA followed by Dunnett's *post hoc* test.
[b] To obtain an infectivity–incubation time standard curve, 10-fold serial dilutions of brain homogenates of mice infected with the Obihiro strain were bioassayed. The 50% lethal dose (LD_{50}) of the original homogenates (10% brain homogenates) was estimated to be 10^6 LD_{50}/20 μl by the Reed-Muench method. The standard curve for incubation periods (x) shorter than 190 days was fitted by the approximation of $LD_{50}=e^{41.48-0.183x}$. The standard curve for incubation periods (x) longer than 190 days was fitted by the approximation of $LD_{50}=e^{21.07-0.076x}$.

Epitope for mAb 6H10

To investigate the epitope for mAb 6H10, we adopted phage display analysis. Fig. 5a shows consensus amino acid (aa) residues deduced from selected phage clones with mAbs 31C6 or 110, or rabbit polyclonal antibodies (pAb) B103. Three or four aa residues of the phage clones selected with mAbs 31C6 and 110 were identical to the aa residues in regions determined by pepspots analysis (Kim et al., 2004a). Similarly, three or four aa residues of selected phage clones with pAb B103 were identical to the synthetic peptide used as the immunogen. These results suggest that at least three residues are required to form an epitope for antibody. In total, 56 phage clones selected after five rounds of panning with mAb 6H10, and these were subjected to DNA sequencing so that the aa sequences could be deduced. The consensus aa residues of two abundant phage clones are listed in Fig. 6a. The most abundant phage clone ph#121 contained four residues identical to the C-terminus of MoPrP (SPSQAWLYMRHE, underlined residues). The second most abundant phage clone ph#125 also had three residues identical to the C-terminus of MoPrP (TQNWSMSMLLKQ, underlined residues). In contrast, no aa sequence identity to MoPrP was observed in the third most abundant phage clone ph#98 (IPLTGKYLDEQS, 6/56, 11%). Binding of antibodies to selected phage clones was confirmed by captured ELISA (Fig. 6b). The mAb 6H10 reacted with phage clones ph#121 and ph#125, originally selected by mAb 6H10, but not with ph#6, originally selected by mAb 31C6. On the other hand, mAb 31C6 reacted only with phage clone ph#6. Taken together, these data demonstrate the specificity of phage clone selection. Moreover, the results suggest that the C-terminus of MoPrP is involved in the formation of the epitope for mAb 6H10. We also analyzed the epitope for mAb 6H10 using a pepspots membrane; however, mAb 6H10 did not react with any spots (data not shown).

Discussion

Immunization of $Prnp^{-/-}$ mice and screening of hybridomas with non-denatured PrP^{Sc} is one of the ways to establish PrP^{Sc}-specific mAbs. Using this approach, we obtained mAb 6H10, which reacted with non-denatured PrP^{Sc} but not with denatured PrP^{Sc}. It is well known that epitopes for pan-PrP antibodies on PrP^{Sc} become accessible by antibodies after dissociation of PrP^{Sc} aggregates and/or denaturation of PrP^{Sc} (Kascsak et al., 1987; Serban et al., 1990; Williamson et al., 1996). However, the reactivity of mAb 6H10 to PrP^{Sc} decreased with the increases in GdnHCl concentration for the pretreatment of PrP^{Sc} to 3 M, indicating that the properties of mAb

a

Antibody: mAb 31C6

aa sequence of epitope	143-DWEDRYYRE-231	
Deduced aa sequences	**DxxxRxxxE** **DWxxR**	(6/11) (2/11)
Possible epitope	**DWEDRYYRE**	

Antibody: mAb 110

aa sequence of epitope	83-PHGGGWG-89	
Deduced aa sequences	**PxGxGW** **PxGxxW**	(6/10) (1/10)
Possible epitope	**PHGGGWG**	

Antibody: pAb B103

aa sequence of epitope	90-QGGTHGQWNKPSKPKTNMK-109	
Deduced aa sequences	**NKxxxP** **HxxxNKxxxP**	(7/11) (2/11)
Possible epitope	QGGTHGQWNKPSKPKTNMK	

Antibody: mAb 6H10

aa sequence of epitope	NA	
Deduced aa sequences	**SQAxxxxR** **TQxxxxS**	(24/56) (13/56)
Possible epitope	213-CVTQYQKESQAYYDGRRSS-231	

b

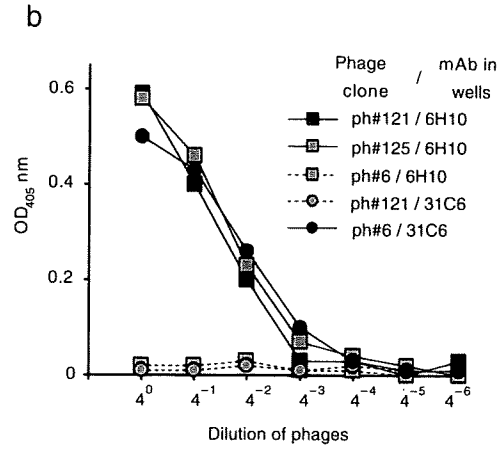

Fig. 6. Epitope analysis by peptide phage display. (a) Identity of aa sequences between selected phage clones and the region to which antibodies are expected to bind. The aa sequence of the epitopes of mAbs 110 and 31C6 were determined by pepspots analysis (Kim et al., 2004a), whereas that of pAb B103 corresponds the synthetic peptide used for immunization (Horiuchi et al., 1995). The deduced aa sequences indicate that consensus aa residues of selected phage clones. Shown are two abundant consensus sequences deduced from selected phage clones, which were obtained after three rounds (for pAb B103, and mAbs 110 and 31C6) or five rounds (for mAb 6H10) of panning. Amino acid residues identical to the expected region are indicated in bold. Numbers in parentheses indicate the total number of phage clones analyzed for each antibody (denominators) and the numbers of phage clones that possess the corresponding consensus aa sequence (numerators). The residues that are expected to constitute the epitope for each antibody are underlined (possible epitope). (b) Binding of antibodies to selected phage clones. Wells coated with mAb 6H10 or 31C6 were incubated with four-fold serial dilutions of the selected phage clones (ph#121, ph#125, or ph#6). Phage–antibody complexes were detected as described in Materials and Methods. Phage clones ph#121 and ph#125, selected by mAb 6H10, express the peptides SPSQAWLYMRHE and TQNWSMSMLLKQ, respectively. Phage ph#6, selected by mAb 31C6, expresses peptide *SDWHTRFHYSMN* (underlining indicates the consensus aa residues for the corresponding epitope).

6H10 differ from those of pan-PrP mAbs. The infectivity of the Obihiro strain, which was used as a source of PrP^{Sc} in this study, was dramatically reduced by the treatment with 3 M GdnHCl (Shindoh et al., 2009), consistent with a decrease in the reactivity of mAb 6H10 to PrP^{Sc} of the Obihiro strain pretreated with 3 M GdnHCl. Furthermore, mAb 6H10 neutralized infectivity of PrP^{Sc} purified from mice infected with the Obihiro strain (Table 1). Thus, mAb 6H10 may recognize a conformational epitope on non-denatured PrP^{Sc} that is related to the oligomerization interface on the PrP^{Sc} molecule. Reduction of the hydrophobic surface on PrP^{Sc} correlated with the dissociation and/or denaturation of PrP^{Sc} by GdnHCl at concentrations between 0 and 3 M (Safar et al., 1994). Circular dichroism analysis also revealed that GdnHCl dissociated PrP^{Sc} aggregates with a midpoint of transition around 2 M (Safar et al., 1993). The half-maximal GdnHCl concentrations, which are required to denature 50% of PrP^{Sc}, have been reported to range from 1.5 to 3 M for most of mouse-adapted scrapie and BSE prions (Legname et al., 2006; Shindoh et al., 2009). In addition, treatment of samples with 2–4 M GdnHCl resulted in decrease of prion infectivity (Caughey et al., 1997; McKenzie et al., 1998). Although these reports used different prion strains, the decrease in reactivity of mAb 6H10 to PrP^{Sc} with an increase in GdnHCl concentration for pretreatment of PrP^{Sc} concurs with structural alteration of PrP^{Sc} or the decrease of infectivity induced by GdnHCl at similar concentrations.

The results of phage display analysis suggested the possibility that the extreme C-terminus of PrP molecule is part of the epitope for mAb 6H10. Among the amino acid residues expected to compose the epitope for mAb 6H10 (aa215-TQxxxxSQAxxxxR-aa228 of MoPrP), the underlined residues are identical to those of sheep and bovine PrP. This may be consistent with the fact that mAb 6H10 could immunoprecipitate PrP^{Sc} from sheep and cattle samples. The mAb 6H10 showed no reaction with denatured PrP^{Sc} by immunoblotting or ELISA (Figs. 1 and 2), or with the corresponding C-terminal peptide by pepspots analysis (data not shown). In contrast, reactivity of mAbs that recognize linear epitopes on the extreme C-terminus increased after pretreatment of PrP^{Sc} with denaturants (Peretz et al., 1997; Kim et al., 2004a). Thus it is unlikely that mAb 6H10 binds linear epitope composed of the C-terminal residues. One mAb, V5B2, which was raised against a synthetic peptide corresponding to the C-terminal residues of human PrP (aa214-CITQYERESQAYY-aa226), is reported to discriminate PrP^{Sc} in brains of CJD patients from PrP^{C} in non-CJD brains possibly by recognizing the oligomerized C-terminal region in PrP^{Sc} oligomers (Curin Serbec et al., 2004; Ulrih et al., 2006). Therefore, the C-terminal regions of two PrP molecules may cooperate to form a conformational epitope; however, the exact properties of the epitope for 6H10 are not yet fully elucidated. Alternatively, in the proposed model of PrP^{Sc} protofibrils, the C-terminal region is thought to be located in close proximity to other regions on the same or different PrP molecule (DeMarco and Daggett, 2004; Govaerts et al., 2004). Cross-linking of recombinant PrP oligomers revealed that an interaction between the N- and C-terminal regions (Kaimann et al., 2008). Thus, the C-terminal region and other regions on the same or different PrP molecule may participate in constituting the epitope for mAb 6H10. The mAb 15B3, which was produced by immunizing recombinant bovine PrP and is purported to be specific to PrP^{Sc}, reacted with three PrP segments, residues 141–147, 161–269, and 213–215 of MoPrP in pepspots analysis (Korth et al., 1997). Involvement of the extreme C-terminus in the epitope for mAb 15B3 is intriguing; however, mAb 6H10 did not react with any PrP peptides in pepspots analysis (data not shown). Thus, the epitope for mAb 6H10 seems to differ from that for mAb 15B3. Recently, mAb 15B3 is reported to react with infectious and non-infectious PrP

aggregates (Biasini et al., 2008), therefore, we analyzed the reactivity of mAb 6H10 to aggregated rMoPrP (Fig. 4). Although a weak non-specific reaction to aggregated rMoPrP was observed, mAb 6H10 did not show any specific reaction to aggregated rMoPrP, suggesting mAb 6H10 is more specific to PrP^{Sc} generated in brains of prion-infected animals.

Some mAbs against either PrP or non-PrP molecules have been reported to immunoprecipitate PrP^{Sc} via an epitope-independent reaction when mAbs were bound to a solid phase such as magnetic beads, as binding of immunoglobulins on the limited area of the solid surface increases the concentration of immunoglobulins in that area and thus a low-affinity interaction between PrP^{Sc} and immunoglobulins on the beads may occur (Morel et al., 2004). We considered that this possibility is unlikely in the case of mAb 6H10 for several reasons. First, bead-free mAb 6H10 reacted with PrP^{Sc} in ELISA and histoblot analysis (Figs. 1 and 5). In addition, a direct interaction of fluorescent dye-labeled mAb 6H10 with non-denatured PrP^{Sc} in brain homogenates of mice infected with prions can be detected in solution by fluorescent correlation spectroscopy (K. S. and M.H., in preparation). Secondly, a Fab' fragment of mAb 6H10 still reacted with native purified PrP^{Sc} in ELISA (data not shown). However, a weak non-specific reaction to aggregated rMoPrP would be expected depending on experimental conditions (Fig. 4), careful experimental design, such as the use of negative control mAb and comparison between prion-infected and mock-infected materials, will be required to ensure specific reactivity of mAb 6H10 to PrP^{Sc}.

The reactivity of mAb 6H10 to PrP^{Sc} in biochemical analysis strongly suggests that mAb 6H10 discriminates PrP^{Sc} from PrP^{C}. However, in histoblot analysis, the mAb showed weak reaction to certain host molecule in *Prnp*$^{-/-}$ mice. This raises two possibilities. First, the mAb may recognize a host molecule other than PrP with an epitope similar to that for mAb 6H10 on PrP^{Sc}. The presence of third abundant phage clone (ph#98) that selected by mAb 6H10, aa sequence of which showed no apparent homology to PrP, may clue the identification of such host molecule. However, no protein or peptide domain was found by homology search using protein blast and tblastn or domain search using Conserved Domain Database. Secondly, the mAb may recognize a host factor tightly associated with PrP^{Sc} in the prion-infected mouse brain, rather than reacting with PrP^{Sc} itself. The latter possibility suggests that the positive reaction to PK-treated PrP^{Sc} in ELISA was due to a reaction to a PK-resistant molecule tightly associated with PrP^{Sc}, which seems unlikely because the PrP^{Sc} fraction used in this study was estimated to be nearly 90% pure after PK treatment (Kim et al., 2004a). However, this possibility cannot be completely ruled out at present, particularly as several macromolecules, including glycosaminoglycans (Snow et al., 1989), ubiquitin (Lowe et al., 1990), apolipoprotein E (Namba et al., 1991) have been shown to co-localize with PrP^{Sc} in brains of prion-infected animals and human. In addition, nucleic acids (Aiken et al., 1990; Sklaviadis et al., 1993) and sphingolipid (Klein et al., 1998) have been co-purified with PrP^{Sc}.

In this study, we showed the possibility that the C-terminal region forms a PrP^{Sc}-specific epitope. Recently, immunization of β-form recombinant human PrP could induce production of mAbs that react with the N-terminal region of PrP^{Sc} (aa91–110; Khalili-Shirazi et al., 2007). The immunization of aggregated synthetic peptide corresponding to aa106–126 of PrP also generated a mAb that discriminates PrP^{Sc} from PrP^{C} (Jones et al., 2009). These results suggest that PrP^{Sc}-specific epitopes are present at various regions on PrP^{Sc}. A fusion protein of PrP and Fc-region of immunoglobulin and PrP-peptide-grafted antibodies have been reported to recognize PrP^{Sc} (Meier et al., 2003; Moroncini et al., 2004, 2006; Solforosi et al., 2007; Lau et al., 2007). In addition, there are nucleotide aptamers that possess higher affinity to PrP^{Sc} than to PrP^{C} (Rhie et al., 2003), and small chemicals such as 9-aminoacridine, streptomycin, luminescent conjugated polymers, polyionic polymers Seprion (Microsens biotechnologies) and others, may also act as PrP^{Sc}-specific probes (Moussa et al., 2006; Phuan et al., 2007; Sigurdson et al., 2007). Despite technical difficulties in manipulating PrP^{Sc} due to its aggregation-prone propensity and heterogeneity, PrP^{Sc}-specific molecular probes are gradually accumulating. As the availability of a panel of anti-PrP mAbs has greatly contributed to characterization of the biochemical properties of PrP, a panel of PrP^{Sc}-specific molecular probes appears to be indispensable tools for analyzing the biochemical and biological properties of native PrP^{Sc} with which prion infectivity is believed to be associated.

Materials and methods

Purification of PrP^{Sc} and production of mAbs

The purification PrP^{Sc} from brains of mice infected with prion Obihiro strain and purity of PrP^{Sc} were reported elsewhere (Kim et al., 2004a). Immunization of PrP^{Sc} and production of mAbs were carried out as described (Kim et al., 2004a).

Antibodies

The following mAbs against mouse PrP molecules were used: 31C6 (IgG1, epitope: aa 143–149), 44B1 (IgG 2a, epitope: aa 155–231), 72 (IgG1, epitope: aa 89–231), and 110 (IgG2b, epitope: aa 59–89) (Kim et al., 2004a). Anti-keyhole limpet hemocyanin (KLH) mAb (IgG2a) and anti-parvovirus mAb P2-168 (IgG2b) (Horiuchi et al., 1997) were used as negative controls. Rabbit antiserum raised against bovine PrP synthetic peptide 103-121 (pAb B103) was also used (Horiuchi et al., 1995). Purification of mAbs was carried out as described elsewhere (Kim et al., 2004a). Conjugation of mAbs with horseradish peroxidase (HRP) was carried out as follows: purified mAbs were digested with pepsin and reduced by 2-mercapthoethanolamine (MEA) to generate Fab' fragments. After removal of MEA with a PD-10 size exclusion column (GE Healthcare), the Fab' fragments were mixed with HRP coupled with the bi-directional cross-linker GMBS (Dojin).

ELISA

Ninety-six well plates (MaxiSorp, Nunc) were coated overnight at 4 °C with either 200 ng purified PrP^{Sc} or 100 ng rMoPrP in 50 μl of 20 mM phosphate buffer (pH 7.0). After adsorption, wells were blocked with 5% fetal bovine serum (FBS) in PBS containing 0.1% Tween 20 (PBST) for 2 h at room temperature (r.t.), and incubated with antibodies diluted with 1% FBS in PBST for 1 h. After washing with PBST, wells were incubated with HRP-conjugated secondary antibodies for 1 h. The antigen–antibody complexes were visualized with 2,2′-azino-bis(3-etht-benzthiazoline-6-sulfonic acid), 0.04% H_2O_2 in 50 mM citrate–phosphate buffer, pH 4.0, and the absorbance at 405 nm was measured with a microplate reader. In some cases, PrP^{Sc} adsorbed to the well was digested with various concentrations of proteinase K (PK) in Tris-buffered saline (TBS; 50 mM Tris–HCl [pH 8.0] and 150 mM NaCl) at 37 °C for 45 min. After terminating PK activity by adding Pefabloc (Roche Diagnostic) to a final concentration at 2 mM, the plates were subjected to the immune reaction.

Immunoblotting

SDS-PAGE and immunoblotting of proteins on an Immobilon-P Transfer Membrane (Millipore) were carried out as described elsewhere (Kim et al., 2004a, 2004b). Membranes were blocked with 5% skim milk in PBST for 1 h and then incubated with HRP-conjugated Fab fragment of anti-PrP mAbs (direct staining) or anti-PrP mAb followed by incubation with HRP-conjugated secondary antibodies (indirect staining). ECL Western blotting detection reagents (GE Healthcare) and X-ray film were used for visualization.

Immunoprecipitation

Protein G-coupled magnetic beads (Dynabeads) were blocked with blocking buffer containing 5% skim milk and 50% Sea Block (Pierce) in PBS. Brain homogenates (2.5%) from prion-infected or uninfected animals were prepared with PBS containing 0.5% I-Block (Applied Biosystem), and were incubated with 10 μg of mAb and protein G magnetic beads for 45 min at 37 °C. The magnetic beads were washed four times with PBS containing 2% Triton X-100 using a magnetic separator. After washing, the beads were suspended with 50 μl of TBS and divided into two tubes. An equal volume of 2 sample buffer (8 M urea, 10% SDS, 8% *b*-mercaptoethanol, 125 mM Tris–HCl [pH 6.8], 6 mM EDTA, 10% glycerol, and 0.04% bromophenol blue) was added to one tube to make samples without PK treatment. The other was treated with 40 μg/ml of PK for 30 min at 37 °C. The reaction with PK was stopped with 2 mM Pefabloc before adding 2 sample buffer.

To examine the reactivity of mAbs to non-infectious PrP aggregates, rMoPrP23-231 or rMoPrP89-231 (Kim et al., 2004a) were diluted to 20 μg/ml with 1 ml of 1% Triton-X 100 in PBS (PBS-Triton, pH 7.2) and kept for 30 min at 20 °C. Then samples were centrifuged at 100,000 × *g* for 45 min at 20 °C. The supernatant was recovered and used as non-aggregated rMoPrP, while the resulting precipitate was resuspended with 1 ml of PBS-Triton by sonication and used as aggregated rMoPrP. Protein G-coupled magnetic beads (100 μl) were incubated with 20 μg of mAbs and then blocked with 5% skim milk and 5% N102 blocking reagent (NOF Corporation, Japan) in PBS-Triton for 1 h at r.t. After washing with PBS-Triton once, the beads were mixed with 300 μl of non-aggregated or aggregated rMoPrP for 45 min at r.t. The beads were washed four times with 1 ml of 2% Triton X-100 in PBS and finally washed with PBS. Proteins bound to the magnetic beads were eluted with 100 μl of 1× sample buffer.

Histoblot analysis

Histoblot analysis was carried out as described by Taraboulos et al. (1992). Immobilon-P Transfer Membranes were activated with methanol and then equilibrated with lysis buffer (0.5% Nonidet P-40, 0.5% sodium deoxycholate, 100 mM NaCl, 10 mM EDTA, 10 mM Tris–HCl [pH 7.8]). Mouse brain cryosections (8 μm) were prepared and placed on glass slides. The glass slides carrying the sections were immediately pressed onto membranes on layers of filter paper saturated with lysis buffer for 1 min. The membranes were thoroughly air-dried and stored at -80 °C until use. Before immunostaining, the membranes were rehydrated in PBST for 1 h at r.t. and then immunostaining was carried out as described above for immunoblotting.

Neutralization of prion infectivity

Fifteen micrograms of purified PrP^{Sc} were incubated with 36 μg of mAb in 300 μl of PBS containing 0.1% Zwittergent 3–12 for 2 h at r.t. The mixture (20 μl) containing 1 μg PrP^{Sc} was then inoculated intracerebrally into 4-week-old female slc:ICR mice. For dose-infectivity correlation, 20 μl each of serially diluted brain homogenates from mice infected with the Obihiro strain were inoculated intracerebrally to 4-week-old female slc:ICR mice.

Peptide phage display

The Ph.D.-12™ Phage Display Library Kit (New England Biolabs), a combinatorial library which expresses random 12-mer-peptides at the N-terminus of a minor coat protein of M13 phage, was used according to the supplier's instructions. Polystyrene Petri dishes (60 × 15 mm) were coated overnight at 4 °C with 1.5 ml of 100 μg/ml antibodies in 0.1 M $NaHCO_3$ (pH 8.6). After blocking with 0.5% FBS in PBS for 1 h, dishes were rinsed six times with PBST and then inoculated with 4×10^{10} of the phage library. After 1 h incubation at r.t., the dishes were washed 10 times with PBS and then bound phage was eluted by addition of 1 ml 0.2 M glycine–HCl (pH 2.2) for 10 min. The eluate was immediately neutralized with 150 μl of 1 M Tris–HCl (pH 9.1). In total, 1 ml of the eluate was used for amplification of the selected phage pool and the amplified phage stock was subsequently used for the next panning.

After three to five rounds of panning, phage DNA encoding the selected random peptide sequences was amplified directly from individual plaques by PCR using primers PD12F (5′-TCAAGCTGTT-TAAGAAATTCACC-3′) and PD12R (5′-TAAAGTTTTGTCGTCTTTCCA-GAC-3′). The PCR products were purified by S-300 HR spin column (GE Healthcare) and used as templates for DNA sequencing. DNA sequences were determined with an automated DNA sequencer (ABI-373A, Applied Biosystems) and using the ABI PRISM Dye Terminator Cycle Sequencing Ready Reaction Kit.

Binding of antibodies to selected peptides was confirmed by a captured ELISA. Briefly, 96-well plates coated with antibodies (20 ng/well) were incubated with four-fold serial dilutions of the phage stock for 1 h at r.t. After washing with PBST, plates were incubated with HRP-conjugated anti-M13 antibody to detect the phage captured by the antibodies. Phage–antibody complexes were detected as described for ELISA.

Pepspots analysis

Pepspots analysis was carried out as described elsewhere (Kim et al., 2004a).

Statistical analysis

Statistical analysis was done with JMP software (SAS Institute Inc.).

Acknowledgments

This work was supported by a grant from the global COE Program (F-001) and a Grant-in-Aid for Science Research (A) (grant 18208026) and a Grant-in-Aid for Exploratory Research (grant 20658070) from the Ministry of Education, Culture, Sports, Science, and Technology of Japan. This work was also supported by a grant from the Ministry of Health, Labour and Welfare of Japan (grant 20330701, Research on Measures for Intractable Diseases). This work was also partly supported by a grant-in-aid from the BSE Control Project of the Ministry of Agriculture, Forestry and Fisheries of Japan, a grant for Strategic Cooperation to Control Emerging and Re-emerging Infections, and the Program of Founding Research Centers for Emerging and Reemerging Infectious Diseases, from the Ministry of Education, Culture, Sports, Science, and Technology, Japan.

References

Aiken, J.M., Williamson, J.L., Borchardt, L.M., Marsh, R.F., 1990. Presence of mitochondrial D-loop DNA in scrapie-infected brain preparations enriched for the prion protein. J. Virol. 64, 3265–3268.

Bessen, R.A., Marsh, R.F., 1994. Distinct PrP properties suggest the molecular basis of strain variation in transmissible mink encephalopathy. J. Virol. 68, 7859–7868.

Biasini, E., Seegulam, M.E., Patti, B.N., Solforosi, L., Medrano, A.Z., Christensen, H.M., Senatore, A., Chiesa, R., Williamson, R.A., Harris, D.A., 2008. Non-infectious aggregates of the prion protein react with several PrP(Sc)-directed antibodies. J. Neurochem. 105, 2190–2204.

Caughey, B.W., Dong, A., Bhat, K.S., Ernst, D., Hayes, S.F., Caughey, W.S., 1991. Secondary structure analysis of the scrapie-associated protein PrP 27-30 in water by infrared spectroscopy. Biochemistry 30, 7672–7680.

Caughey, B., Raymond, G.J., Kocisko, D.A., Lansbury Jr., P.T., 1997. Scrapie infectivity correlates with converting activity, protease resistance, and aggregation of scrapie-associated prion protein in guanidine denaturation studies. J. Virol. 71, 4107–4110.

Curin Serbec, V., Bresjanac, M., Popovic, M., Pretnar Hartman, K., Galvani, V., Rupreht, R., Cernilec, M., Vranac, T., Hafner, I., Jerala, R., 2004. Monoclonal antibody against a peptide of human prion protein discriminates between Creutzfeldt-Jacob's disease-affected and normal brain tissue. J. Biol. Chem. 279, 3694–3698.

DeMarco, M.L., Daggett, V., 2004. From conversion to aggregation: protofibril formation of the prion protein. Proc. Natl. Acad. Sci. U.S.A. 101, 2293–2298.
Enari, M., Flechsig, E., Weissmann, C., 2001. Scrapie prion protein accumulation by scrapie-infected neuroblastoma cells abrogated by exposure to a prion protein antibody. Proc. Natl. Acad. Sci. U.S.A. 98, 9295–9299.
Fischer, M.B., Roeckl, C., Parizek, P., Schwarz, H.P., Aguzzi, A., 2000. Binding of disease-associated prion protein to plasminogen. Nature 408, 479–483.
Govaerts, C., Wille, H., Prusiner, S.B., Cohen, F.E., 2004. Evidence for assembly of prions with left-handed beta-helices into trimers. Proc. Natl. Acad. Sci. U.S.A. 101, 8342–8347.
Horiuchi, M., Yamazaki, N., Ikeda, T., Ishiguro, N., Shinagawa, M., 1995. A cellular form of prion protein (PrPC) exists in many non-neuronal tissues of sheep. J. Gen. Virol. 76, 2583–2587.
Horiuchi, M., Mochizuki, M., Ishiguro, N., Nagasawa, H., Shinagawa, M., 1997. Epitope mapping of a monoclonal antibody specific to feline panleukopenia virus and mink enteritis virus. J. Vet. Med. Sci. 59, 133–136.
Horiuchi, M., Chabry, J., Caughey, B., 1999. Specific binding of normal prion protein to the scrapie form via a localized domain initiates its conversion to the protease-resistant state. EMBO J. 18, 3193–3203.
Jones, M., Wight, D., McLoughlin, V., Norrby, K., Ironside, J.W., Connolly, J.G., Farquhar, C.F., MacGregor, I.R., Head, M.W., 2009. An antibody to the aggregated synthetic prion protein peptide (PrP106-126) selectively recognizes disease-associated prion protein (PrP) from human brain specimens. Brain Pathol. 19, 293–302.
Kaimann, T., Metzger, S., Kuhlmann, K., Brandt, B., Birkmann, E., Höltje, H.D., Riesner, D., 2008. Molecular model of an alpha-helical prion protein dimer and its monomeric subunits as derived from chemical cross-linking and molecular modeling calculations. J. Mol. Biol. 376, 582–596.
Kascsak, R.J., Rubenstein, R., Merz, P.A., Tonna-DeMasi, M., Fersko, R., Carp, R.I., Wisniewski, H.M., Diringer, H., 1987. Mouse polyclonal and monoclonal antibody to scrapie-associated fibril proteins. J. Virol. 61, 3688–3693.
Khalili-Shirazi, A., Kaisar, M., Mallinson, G., Jones, S., Bhelt, D., Fraser, C., Clarke, A.R., Hawke, S.H., Jackson, G.S., Collinge, J., 2007. Beta-PrP form of human prion protein stimulates production of monoclonal antibodies to epitope 91-110 that recognise native PrPSc. Biochim. Biophys. Acta 1774, 1438–1450.
Kim, C.L., Umetani, A., Matsui, T., Ishiguro, N., Shinagawa, M., Horiuchi, M., 2004a. Antigenic characterization of an abnormal isoform of prion protein using a new diverse panel of monoclonal antibodies. Virology 320, 40–51.
Kim, C.L., Karino, A., Ishiguro, N., Shinagawa, M., Sato, M., Horiuchi, M., 2004b. Cell-surface retention of PrPC by anti-PrP antibody prevents protease-resistant PrP formation. J. Gen. Virol. 85, 3473–3482.
Klein, T.R., Kirsch, D., Kaufmann, R., Riesner, D., 1998. Prion rods contain small amounts of two host sphingolipids as revealed by thin-layer chromatography and mass spectrometry. Biol. Chem. 379, 655–666.
Korth, C., Stierli, B., Streit, P., Moser, M., Schaller, O., Fischer, R., Schulz-Schaeffer, W., Kretzschmar, H., Raeber, A., Braun, U., Ehrensperger, F., Hornemann, S., Glockshuber, R., Riek, R., Billeter, M., Wüthrich, K., Oesch, B., 1997. Prion (PrPSc)-specific epitope defined by a monoclonal antibody. Nature 390, 74–77.
Lau, A.L., Yam, A.Y., Michelitsch, M.M., Wang, X., Gao, C., Goodson, R.J., Shimizu, R., Timoteo, G., Hall, J., Medina-Selby, A., Coit, D., McCoin, C., Phelps, B., Wu, P., Hu, C., Chien, D., Peretz, D., 2007. Characterization of prion protein (PrP)-derived peptides that discriminate full-length PrPSc from PrPC. Proc. Natl. Acad. Sci. U.S.A. 104, 11551–11556.
Legname, G., Nguyen, H.O., Peretz, D., Cohen, F.E., DeArmond, S.J., Prusiner, S.B., 2006. Continuum of prion protein structures enciphers a multitude of prion isolate-specified phenotypes. Proc. Natl. Acad. Sci. U.S.A. 103, 19105–19110.
Lowe, J., McDermott, H., Kenward, N., Landon, M., Mayer, R.J., Bruce, M., McBride, P., Somerville, R.A., Hope, J., 1990. Ubiquitin conjugate immunoreactivity in the brains of scrapie infected mice. J. Pathol. 162, 61–66.
McKenzie, D., Bartz, J., Mirwald, J., Olander, D., Marsh, R., Aiken, J., 1998. Reversibility of scrapie inactivation is enhanced by copper. J. Biol. Chem. 273, 25545–25547.
Meier, P., Genoud, N., Prinz, M., Maissen, M., Rülicke, T., Zurbriggen, A., Raeber, A.J., Aguzzi, A., 2003. Soluble dimeric prion protein binds PrP(Sc) in vivo and antagonizes prion disease. Cell 113, 49–60.
Meyer, R.K., McKinley, M.P., Bowman, K.A., Braunfeld, M.B., Barry, R.A., Prusiner, S.B., 1986. Separation and properties of cellular and scrapie prion proteins. Proc. Natl. Acad. Sci. U.S.A. 83, 2310–2314.
Morel, N., Simon, S., Frobert, Y., Volland, H., Mourton-Gilles, C., Negro, A., Sorgato, M.C., Créminon, C., Grassi, J., 2004. Selective and efficient immunoprecipitation of the disease-associated form of the prion protein can be mediated by nonspecific interactions between monoclonal antibodies and scrapie-associated fibrils. J. Biol. Chem. 279, 30143–30149.
Moroncini, G., Kanu, N., Solforosi, L., Abalos, G., Telling, G.C., Head, M., Ironside, J., Brockes, J.P., Burton, D.R., Williamson, R.A., 2004. Motif-grafted antibodies containing the replicative interface of cellular PrP are specific for PrPSc. Proc. Natl. Acad. Sci. U.S.A. 101, 10404–10409.
Moroncini, G., Mangieri, M., Morbin, M., Mazzoleni, G., Ghetti, B., Gabrielli, A., Williamson, R.A., Giaccone, G., Tagliavini, F., 2006. Pathologic prion protein is specifically recognized in situ by a novel PrP conformational antibody. Neurobiol. Dis. 23, 717–724.
Moussa, A., Coleman, A.W., Bencsik, A., Leclere, E., Perret, F., Martin, A., Perron, H., 2006. Use of streptomycin for precipitation and detection of proteinase K resistant prion protein (PrPsc) in biological samples. Chem. Commun. 9, 973–975.
Namba, Y., Tomonaga, M., Kawasaki, H., Otomo, E., Ikeda, K., 1991. Apolipoprotein E immunoreactivity in cerebral amyloid deposits and neurofibrillary tangles in Alzheimer's disease and kuru plaque amyloid in Creutzfeldt-Jakob disease. Brain Res. 541, 163–166.
Oesch, B., Westaway, D., Wälchli, M., McKinley, M.P., Kent, S.B., Aebersold, R., Barry, R.A., Tempst, P., Teplow, D.B., Hood, L.E., Prusiner, S.B., Weissmann, C., 1985. A cellular gene encodes scrapie PrP 27-30 protein. Cell 40, 735–746.
Pan, K.M., Baldwin, M., Nguyen, J., Gasset, M., Serban, A., Groth, D., Mehlhorn, I., Huang, Z., Fletterick, R.J., Cohen, F.E., Prusiner, S.B., 1993. Conversion of alpha-helices into beta-sheets features in the formation of the scrapie prion proteins. Proc. Natl. Acad. Sci. U.S.A. 90, 10962–10966.
Paramithiotis, E., Pinard, M., Lawton, T., LaBoissiere, S., Leathers, V.L., Zou, W.Q., Estey, L.A., Lamontagne, J., Lehto, M.T., Kondejewski, L.H., Francoeur, G.P., Papadopoulos, M., Haghighat, A., Spatz, S.J., Head, M., Will, R., Ironside, J., O'Rourke, K., Tonelli, Q., Ledebur, H.C., Chakrabartty, A., Cashman, N.R., 2003. A prion protein epitope selective for the pathologically misfolded conformation. Nat. Med. 9, 893–899.
Peretz, D., Williamson, R.A., Matsunaga, Y., Serban, H., Pinilla, C., Bastidas, R.B., Rozenshteyn, R., James, T.L., Houghten, R.A., Cohen, F.E., Prusiner, S.B., Burton, D.R., 1997. A conformational transition at the N terminus of the prion protein features in formation of the scrapie isoform. J. Mol. Biol. 273, 614–622.
Peretz, D., Williamson, R.A., Kaneko, K., Vergara, J., Leclerc, E., Schmitt-Ulms, G., Mehlhorn, I.R., Legname, G., Wormald, M.R., Rudd, P.M., Dwek, R.A., Burton, D.R., Prusiner, S.B., 2001. Antibodies inhibit prion propagation and clear cell cultures of prion infectivity. Nature 412, 739–743.
Perrier, V., Solassol, J., Crozet, C., Frobert, Y., Mourton-Gilles, C., Grassi, J., Lehmann, S., 2004. Anti-PrP antibodies block PrPSc replication in prion-infected cell cultures by accelerating PrPC degradation. J. Neurochem. 89, 454–463.
Phuan, P.W., Zorn, J.A., Safar, J., Giles, K., Prusiner, S.B., Cohen, F.E., May, B.C., 2007. Discriminating between cellular and misfolded prion protein by using affinity to 9-aminoacridine compounds. J. Gen. Virol. 88, 1392–1401.
Prusiner, S.B., Scott, M.R., DeArmond, S.J., Cohen, F.E., 1998. Prion protein biology. Cell 93, 337–348.
Rhie, A., Kirby, L., Sayer, N., Wellesley, R., Disterer, P., Sylvester, I., Gill, A., Hope, J., James, W., Tahiri-Alaoui, A., 2003. Characterization of 2′-fluoro-RNA aptamers that bind preferentially to disease-associated conformations of prion protein and inhibit conversion. J. Biol. Chem. 278, 39697–39705.
Safar, J., Roller, P.P., Gajdusek, D.C., Gibbs Jr., C.J., 1993. Conformational transitions, dissociation, and unfolding of scrapie amyloid (prion) protein. J. Biol. Chem. 268, 20276–20284.
Safar, J., Roller, P.P., Gajdusek, D.C., Gibbs Jr., C.J., 1994. Scrapie amyloid (prion) protein has the conformational characteristics of an aggregated molten globule folding intermediate. Biochemistry 33, 8375–8383.
Safar, J., Wille, H., Itri, V., Groth, D., Serban, H., Torchia, M., Cohen, F.E., Prusiner, S.B., 1998. Eight prion strains have PrP(Sc) molecules with different conformations. Nat. Med. 4, 1157–1165.
Safar, J.G., Geschwind, M.D., Deering, C., Didorenko, S., Sattavat, M., Sanchez, H., Serban, A., Vey, M., Baron, H., Giles, K., Miller, B.L., Dearmond, S.J., Prusiner, S.B., 2005. Diagnosis of human prion disease. Proc. Natl. Acad. Sci. U.S.A. 102, 3501–3506.
Serban, D., Taraboulos, A., DeArmond, S.J., Prusiner, S.B., 1990. Rapid detection of Creutzfeldt-Jakob disease and scrapie prion proteins. Neurology 40, 110–117.
Shindoh, R., Kim, C.L., Song, C.H., Hasebe, R., Horiuchi, M., 2009. The region approximately between amino acids 81 and 137 of proteinase K-resistant PrPSc is critical for the infectivity of the chandler prion strain. J. Virol. 83, 3852–3860.
Sigurdson, C.J., Nilsson, K.P., Hornemann, S., Manco, G., Polymenidou, M., Schwarz, P., Leclerc, M., Hammarström, P., Wüthrich, K., Aguzzi, A., 2007. Prion strain discrimination using luminescent conjugated polymers. Nat. Methods 4, 1023–1030.
Silveira, J.R., Raymond, G.J., Hughson, A.G., Race, R.E., Sim, V.L., Hayes, S.F., Caughey, B., 2005. The most infectious prion protein particles. Nature 437, 257–261.
Sklaviadis, T., Akowitz, A., Manuelidis, E.E., Manuelidis, L., 1993. Nucleic acid binding proteins in highly purified Creutzfeldt-Jakob disease preparations. Proc. Natl. Acad. Sci. U.S.A. 90, 5713–5717.
Snow, A.D., Kisilevsky, R., Willmer, J., Prusiner, S.B., DeArmond, S.J., 1989. Sulfated glycosaminoglycans in amyloid plaques of prion diseases. Acta Neuropathol. 77, 337–342.
Solforosi, L., Bellon, A., Schaller, M., Cruite, J.T., Abalos, G.C., Williamson, R.A., 2007. Toward molecular dissection of PrPC-PrPSc interactions. J. Biol. Chem. 282, 7465–7471.
Ulrih, N.P., Skrt, M., Veranic, P., Galvani, V., Vranac, T., Curin Serbec, V., 2006. Oligomeric forms of peptide fragment PrP(214-226) in solution are preferentially recognized by PrP(Sc)-specific antibody. Biochem. Biophys. Res. Commun. 344, 1320–1326.
Taraboulos, A., Jendroska, K., Serban, D., Yang, S.L., DeArmond, S.J., Prusiner, S.B., 1992. Regional mapping of prion proteins in brain. Proc. Natl. Acad. Sci. U.S.A. 89, 7620–7624.
Williamson, R.A., Peretz, D., Smorodinsky, N., Bastidas, R., Serban, H., Mehlhorn, I., DeArmond, S.J., Prusiner, S.B., Burton, D.R., 1996. Circumventing tolerance to generate autologous monoclonal antibodies to the prion protein. Proc. Natl. Acad. Sci. U.S.A. 93, 7279–7282.

JOURNAL OF VIROLOGY, Apr. 2009, p. 3852–3860 Vol. 83, No. 8
0022-538X/09/$08.00+0 doi:10.1128/JVI.01740-08
Copyright © 2009, American Society for Microbiology. All Rights Reserved.

The Region Approximately between Amino Acids 81 and 137 of Proteinase K-Resistant PrP^{Sc} Is Critical for the Infectivity of the Chandler Prion Strain▽

Ryo Shindoh, Chan-Lan Kim,† Chang-Hyun Song, Rie Hasebe, and Motohiro Horiuchi*

Laboratory of Prion Diseases, Graduate School of Veterinary Medicine, Hokkaido University, Kita 18, Nishi 9, Kita-ku, Sapporo 060-0818, Japan

Received 17 August 2008/Accepted 16 January 2009

Although the major component of the prion is believed to be the oligomer of PrP^{Sc}, little information is available concerning regions on the PrP^{Sc} molecule that affect prion infectivity. During the analysis of PrP^{Sc} molecules from various prion strains, we found that PrP^{Sc} of the Chandler strain showed a unique property in the conformational-stability assay, and this property appeared to be useful for studying the relationship between regions of the PrP^{Sc} molecule and prion infectivity. Thus, we analyzed PrP^{Sc} of the Chandler strain in detail and analyzed the infectivities of the N-terminally denatured and truncated forms of proteinase K-resistant PrP. The N-terminal region of PrP^{Sc} of the Chandler strain showed region-dependent resistance to guanidine hydrochloride (GdnHCl) treatment. The region approximately between amino acids (aa) 81 and 137 began to be denatured by treatment with 1.5 M GdnHCl. Within this stretch, the region comprising approximately aa 81 to 90 was denatured almost completely by 2 M GdnHCl. Furthermore, the region approximately between aa 90 and 137 was denatured completely by 3 M GdnHCl. However, the C-terminal region thereafter was extremely resistant to the GdnHCl treatment. This property was not observed in PrP^{Sc} molecules of other prion strains. Denaturation of the region between aa 81 and 137 by 3 M GdnHCl significantly prolonged the incubation periods in mice compared to that for the untreated control. More strikingly, the denaturation and removal of this region nearly abolished the infectivity. This finding suggests that the conformation of the region between aa 81 and 137 of the Chandler strain PrP^{Sc} molecule is directly associated with prion infectivity.

Prion diseases, such as scrapie, bovine spongiform encephalopathy (BSE), and Creutzfeldt-Jakob disease, are fatal neurodegenerative disorders characterized by the accumulation of a disease-specific, abnormal isoform of the prion protein, PrP^{Sc}, in the central nervous system, astrogliosis, neuronal vacuolation, and neuronal cell death. PrP^{Sc} is believed to be generated from a cellular form of prion protein, PrP^{C}, by a posttranslational modification including conformational transformation. Although the prion entity, the causative agent of prion diseases, remains to be elucidated, PrP^{Sc} is believed to be a major component of the prion.

Direct interaction between PrP^{C} and preexisting PrP^{Sc} precedes the transformation of PrP^{C} into newly generated PrP^{Sc}. Data on the regions of PrP^{C} that are indispensable for PrP^{Sc} formation and prion propagation have been accumulated using neuroblastoma cells persistently infected with prions and transgenic (Tg) mice expressing mutant PrPs. Although the extreme N-terminal region, amino acids (aa) 23 to 32, modulates prion propagation (8, 9, 34), the region between aa 32 and approximately aa 90 is not essential for the production of PrP^{Sc} and the propagation of the prion (9, 18, 22, 39). The region of residues 114 to 121, the most amyloidgenic region of PrP, is essential for the conversion of PrP^{C} into PrP^{Sc} (11, 23). A deletion mutant lacking residues 23 to 88 and 141 to 176 can convert into PrP^{Sc} and support prion propagation in Tg mice, suggesting that the region of residues 141 to 176 is not essential for prion propagation (22, 34). The cysteine residue at 178 that forms an intramolecular disulfide bond with another cysteine residue at 213 is essential for PrP^{Sc} formation (22). Additionally, amino acid substitutions at 167 and 218 prevent PrP^{Sc} formation and show a dominant-negative effect on prion propagation (15, 28). Due to the difficulty of direct manipulation of PrP^{Sc}, the regions of PrP^{Sc} that are important for prion infectivity have not been elucidated. It is well accepted that not the removal of the protease-sensitive N-terminal domain (aa 23 to around aa 90) from PrP^{Sc} but the denaturation of the remaining C-terminal domain diminishes prion infectivity. However, the relationship between prion infectivity and the regions of PrP^{Sc} is largely unclear.

From the analysis of biochemical properties of PrP^{Sc} molecules of various prion strains, we found that PrP^{Sc} of the Chandler strain has region-dependent resistance to denaturation by guanidine hydrochloride (GdnHCl). This property allows for the denaturation and removal of specific regions of PrP^{Sc}. In this study, we describe the unique conformational stability of PrP^{Sc} of the Chandler strain and demonstrate that the region approximately between aa 81 and 137 of PrP^{Sc} is important for the infectivity of the Chandler prion strain.

MATERIALS AND METHODS

Mouse and prion strains. Mouse-adapted prion strains 22L (7), Chandler (17), Fukuoka-1 (35), G1 (unpublished data), and Obihiro (31) were used in this study. These mouse-adapted strains were propagated in female Jcl:ICR mice (CLEA

* Corresponding author. Present address: Laboratory of Prion Diseases, Graduate School of Veterinary Medicine, Hokkaido University, Kita 18, Nishi 9, Kita-ku, Sapporo 060-0818, Japan. Phone and fax: 81-11-706-5293. E-mail: horiuchi@vetmed.hokudai.ac.jp.

† Present address: Foreign Animal Disease Division, Animal Disease Control Department, National Veterinary Research and Quarantine Service, 480 Anyang-6 dong, Manan-gu, Anyang 430-824, Republic of Korea.

▽ Published ahead of print on 28 January 2009.

Japan) except where otherwise specified. In some cases, C56BL/6J mice (CLEA Japan) and RIII/J and I/LnJ mice (Jackson Laboratories) were used for prion propagation. In addition, mouse-adapted BSE prion strains, designated KUS-m and TE-m, which were derived from samples obtained in Japanese BSE cases KUS and TE by a third serial passage in RIII/J and C57BL/6J mice, respectively, were used. All procedures for animal experiments were carried out according to protocols approved by the Institutional Committee for Animal Experiments.

Antibodies. Anti-PrP monoclonal antibodies (MAbs) 110, 118, 147, 31C6, 43C5, and 44B1 (16) were used. In addition, B103 rabbit polyclonal antibodies (pAb) raised against the bovine PrP synthetic peptide comprising aa 103 to 121, which corresponds to aa 90 to 109 of mouse PrP, were used (13).

Conformational-stability assay. Conformational-stability assays were carried out as described by Legname et al. (19, 20) with some modifications. The brains of mice infected with prions were homogenized in phosphate-buffered saline (PBS) to make 10% homogenates. Aliquots of the homogenates were stored at −30°C until use. The 10% brain homogenates (50 μl) were mixed with equal volumes of various concentrations of GdnHCl (0 to 8 M) and incubated at 37°C for 1 h. Samples were then diluted by the addition of 850 μl of NTS buffer (10 mM Tris-HCl [pH 8.0], 150 mM NaCl, 0.5% Triton X-100, and 0.5% sodium deoxycholate). To adjust the final GdnHCl concentration to 0.4 M, 50 μl of various concentrations of GdnHCl (0 to 8 M) were added to the samples. The samples were then digested with proteinase K (PK; Roche) at 20 μg/ml for 30 min at 37°C. After the termination of PK activity by adding Pefabloc (Roche) to obtain a final concentration of 2 mM, 500 μl of a 5:1 mixture of 2-butanol and methanol was added and the samples were mixed well and kept for 10 min at ambient temperature. PrP^{Sc} was pelleted by centrifugation at 20,000 × *g* for 10 min at 20°C. The resulting pellet was dissolved in 1× sodium dodecyl sulfate (SDS) sample buffer (62.5 mM Tris-HCl [pH 6.8], 5% glycerol, 3 mM EDTA, 4% β-mercaptoethanol, 0.04% bromophenol blue, 5% SDS, 4 M urea) by being boiled for 5 min. SDS-polyacrylamide gel electrophoresis and immunoblotting were carried out as described elsewhere (38). The chemiluminescence intensities of bands of PrP^{Sc} were measured with a LAS-3000 chemiluminescence image analyzer (Fujifilm). Quantitative analyses of the blots were carried out with Image Reader LAS-3000 software, version 1.11 (Fujifilm). The sigmoidal patterns of denaturation curves were plotted using a nonlinear least-squares fit. The concentrations of GdnHCl required to denature 50% of PrP^{Sc} ($[GdnHCl]_{1/2}$ values) were estimated from the denaturation curves, and statistical analysis was carried out by a one-way analysis of variance followed by a Newman-Keuls test.

Deglycosylation. The 10% brain homogenates (250 μl) were mixed with equal volumes of the NTS buffer and digested with PK at 20 μg/ml for 1 h at 37°C. Proteolysis was terminated by the addition of Pefabloc to a final concentration of 4 mM. Samples were then mixed with 1/5 volume of 5× denaturation buffer (20 mM Tris-HCl [pH 7.5], 150 mM NaCl, 2 mM EDTA, 5% SDS, 10% β-mercaptoethanol) and 5 U of *N*-glycosidase F (Roche) and incubated for 16 h at 37°C. Proteins were precipitated by the addition of 1/2 volume of a 5:1 mixture of 2-butanol and methanol followed by centrifugation at 20,000 × *g* for 10 min at 20°C.

Preparation of cell lysates. A Neuro2a mouse neuroblastoma subclone persistently infected with the Chandler strain (ScN2a-5) (38) was used. ScN2a-5 cells grown in 10-cm dishes were collected by using a cell scraper and pelleted by centrifugation at 300 × *g* for 5 min. The cells were washed once with PBS and pelleted again by centrifugation. The resulting pellets were lysed with 1 ml of lysis buffer (10 mM Tris-HCl [pH 7.5], 0.5% Triton X-100, 0.5% sodium deoxycholate, 150 mM NaCl, 5 mM EDTA) for 30 min on ice. Nuclei and cell debris were removed by low-speed centrifugation at 300 × *g*, and supernatants were further centrifuged at 100,000 × *g* for 30 min at 4°C. The resulting pellets were suspended in 50 μl of PBS and used for conformational-stability assays as the PrP^{Sc}-enriched fraction.

Bioassay. The 10% brain homogenates (540 μl) were mixed with equal volumes of various concentrations (0 to 6 M) of GdnHCl solution and then incubated at 37°C for 1 h. Samples were then diluted by the addition of 9.18 ml of NTS buffer, and 540 μl of various concentrations of GdnHCl solution were added to adjust the final concentration of GdnHCl to 0.4 M. The mixtures were ultracentrifuged at 197,000 × *g* for 2.5 h at 4°C, and the resulting pellet was resuspended in 540 μl of PBS and used for the bioassay. Small aliquots of the samples were digested with PK and analyzed by immunoblotting to confirm the existence of PrP^{Sc}. To prepare the PK-treated inoculums for the bioassay, 540-μl aliquots of 10% brain homogenates were treated with GdnHCl as described above. After the GdnCHl treatment, samples were digested with 10 μg/ml of PK for 1 h at 37°C, and digestion was stopped by adding Pefabloc to a final concentration of 2 mM. Samples were ultracentrifuged, and the resulting pellets were resuspended in PBS as described above. Samples (20 μl) were intracerebrally inoculated into 4-week-old female Jcl:ICR mice.

RESULTS

Conformational stabilities of PrP^{Sc} molecules of the mouse-adapted prion strains. To examine the biochemical differences of PrP^{Sc} molecules from various mouse-adapted prion strains, conformational-stability assays were carried out to assess the resistance of PrP^{Sc} to denaturation by GdnHCl (Fig. 1A). When immunoblots were probed with pAb B103 and MAb 44B1, which recognize aa 90 to 109 and aa 155 to 231 of mouse PrP, respectively, the amounts of PrP^{Sc} molecules of the G1, Obihiro, and Fukuoka-1 strains were found to be nearly unchanged by treatment with up to 2 M GdnHCl. The treatment with 2.5 M GdnHCl led to the first decrease in the amount of PrP^{Sc}, and only a trace amount of PrP^{Sc} was detected after treatment with 3 M GdnHCl. The $[GdnHCl]_{1/2}$ was estimated from the denaturation curve for each prion strain (Fig. 1A). The $[GdnHCl]_{1/2}$ values for the G1, Obihiro, and Fukuoka-1 strains based on the results obtained with MAb 44B1 ranged from 2.0 to 2.1 M, and there was no significant difference among them (Table 1). This finding indicates that these strains have similar levels of resistance to GdnHCl treatment. In contrast, the $[GdnHCl]_{1/2}$ for the 22L strain was significantly lower than those for the G1, Obihiro, and Fukuoka-1 strains, indicating that PrP^{Sc} of the 22L strain is less stable than those of other strains. Moreover, the $[GdnHCl]_{1/2}$ values for BSE strains KUS-m and TE-m were higher than those for other mouse-adapted prion strains except the Chandler strain. The incubation period for each prion strain and the $[GdnHCl]_{1/2}$ values are summarized in Table 1. Although the $[GdnHCl]_{1/2}$ values for the G1, Obihiro, and Fukuoka-1 strains are comparable, the G1 strain had an extremely long incubation period.

Among the PrP^{Sc} molecules of the prion strains used in this study, PrP^{Sc} of the Chandler strain showed a unique alteration in molecular mass with the increase of the GdnHCl concentration. When the blots were probed with pAb B103, the PrP^{Sc} bands detected in the samples treated with 2.0 and 2.5 M GdnHCl were approximately 1 to 2 kDa smaller than those in samples treated with lower concentrations, and PrP^{Sc} was almost undetectable after the 3 M GdnHCl treatment. When the blots were probed with MAb 44B1, the PrP^{Sc} bands detected in samples treated with more than 2.0 M GdnHCl were approximately 6 to 7 kDa smaller than those in samples treated with lower concentrations, and these bands were still detected even after the treatment with 3.5 M GdnHCl. The $[GdnHCl]_{1/2}$ for PrP^{Sc} of the Chandler strain was estimated to be 3.2 M from the results obtained with MAb 44B1.

Further characterization of the GdnHCl resistance of PrP^{Sc} of the Chandler strain. The results of the conformational-stability assays suggested that the N- and C-terminal regions of PK-resistant PrP^{Sc} of the Chandler strain have different levels of resistance to GdnHCl treatment. Thus, we analyzed PrP^{Sc} of the Chandler strain more precisely with six additional MAbs (Fig. 2). By using MAb 110, recognizing repetitive amino acid sequences at positions 59 to 65 and 83 to 89, PrP^{Sc} was undetected after treatments with more than 2 M GdnHCl. The major N terminus of the PK-resistant core of PrP^{Sc} molecules (designated PrP27-30) of the ME7 and Obihiro strains is reported to be Gly at position 81 (10, 12). Moreover, the molecular mass of deglycosylated Chandler PrP^{Sc} is identical to that of the Obihiro strain PrP^{Sc} (Fig. 1B). Taken together, these

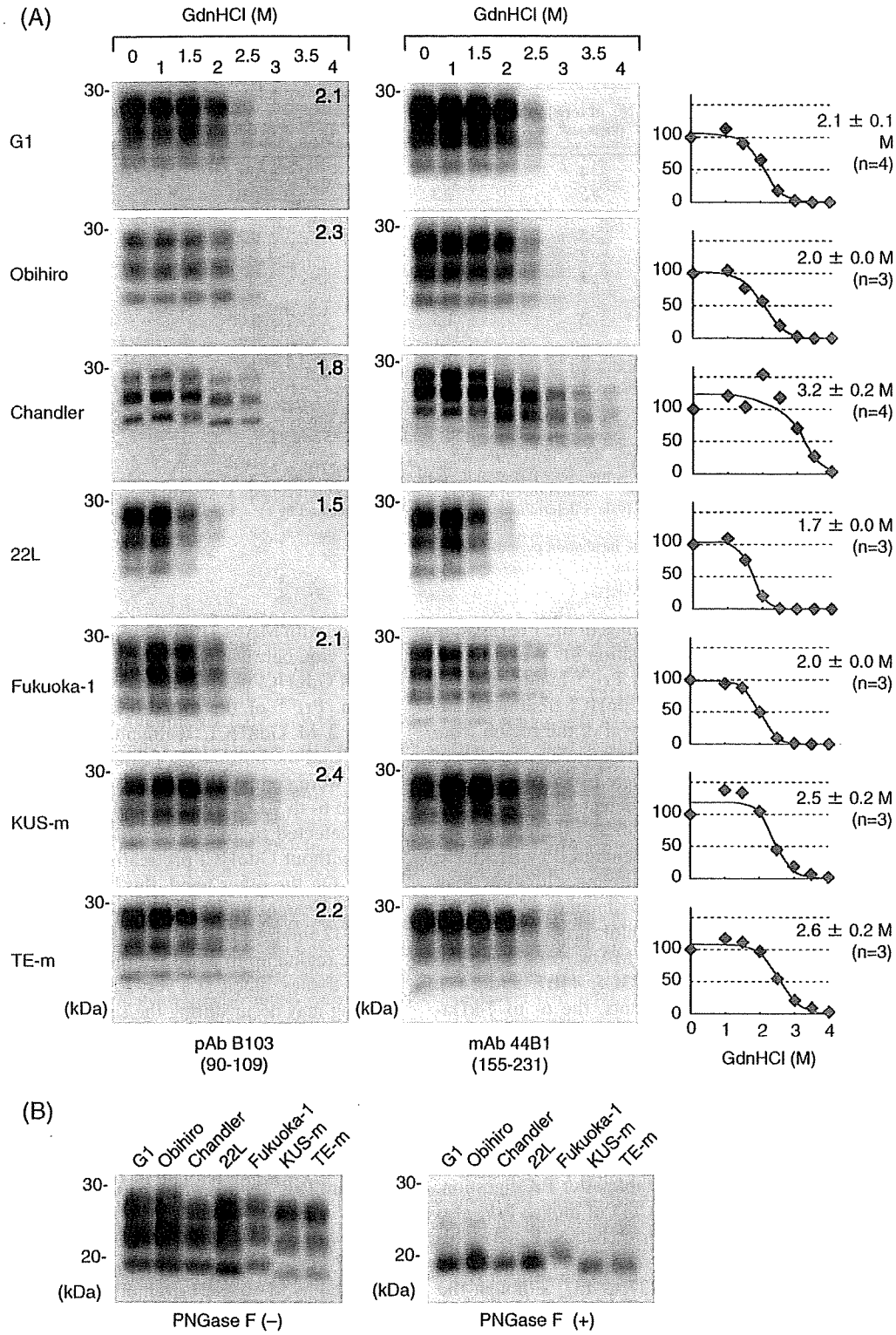

FIG. 1. Conformational stabilities of PrP^{Sc} molecules of various prion strains. (A) Immunoblots for the conformational-stability assay. Brain homogenates from prion-infected mice (prion strains are indicated to the left) were treated with 0 to 4 M GdnHCl (as indicated at the top) and subjected to PK digestion. PrP^{Sc} was detected by either pAb B103 (left column) or MAb 44B1 (right column). Epitopes for antibodies are indicated in parentheses. Independent assays of each strain with MAb 44B1 were carried out at least three times (the number of assays is indicated in parentheses to the right of the graphs), and based on the quantitative results for the blots probed with MAb 44B1, the denaturation curves were plotted using a nonlinear least-squares fit. $[GdnHCl]_{1/2}$ values (means ± SD) are indicated for each graph. Numbers in the top right corners of the blots probed with pAb B103 are the $[GdnHCl]_{1/2}$ values (in molars). (B) Molecular masses of PrP^{Sc} molecules. Brain homogenates from prion-infected mice (prion strains are indicated at the top) were treated with PK, and the immunoblot was probed with pAb B103. To compare the molecular masses of the PK-resistant cores of PrP^{Sc} molecules more precisely, PK-treated samples were further treated with peptide-*N*-glycosidase F (PNGase F) (right). −, absent; +, present.